Check for
updates

Progress in mechanism design of functional composites for anti-ice/deicing materials

Zhongxian Zhao[1,2], Xiaofeng Li[1], Wenge Li[3], Minghui Liu[4], Zhaowei Hu[2], Tao Jiang[3], Haoran Wang[3] and Yuantao Zhao[3*]

Abstract

Icing as a regular natural phenomenon in life poses a serious threat to human production and life, traditional mechanical deicing, chemical deicing, and other methods have the shortcomings of high pollution, high energy consumption, and low efficiency, which limits their applicability and effectiveness of the scene of the above methods. With the expansion of global economic activities in recent years, the solution to the icing problem has become imminent. As a result, researchers have gradually deepened their studies related to anti-icing. Inspired by the lotus leaf effect, hogwash, polar, marine shellfish, and other natural organisms, anti-icing/deicing coatings can be designed functional biomimetic through both surface micro-nano structures and the physicochemical properties of the material. Superhydrophobic design is based on Young's wetting equations, Wenzel's wetting equations, and the Cassie-Baxter model of the superhydrophobic behavior of the interface formed by the liquid droplets and the surface, which prevents the droplets from spreading out and penetration to form heat exchange. The physicochemical properties are based on the slow-release behavior of chemical mediators inside the coating with properties such as super-lubrication and anti-freezing, which reduce the residence time and nucleation temperature of droplets on the surface. The coating effectively blocks the occurrence of icing behavior by passive means such as ultra-low interfacial wetting, interfacial slip, and lowering the freezing point of droplets, which has become a hot research direction. Meanwhile, the active anti-icing of photo-thermal, electro-thermal, phase change and other effects with the passive anti-icing to play a synergistic and complementary role for further enhance the anti-icing effect of the coating. To clarity the design mechanism and preparation process of the anti-icing/ice-removing surfaces, the article firstly classifies and introduces the coatings functioned according to the different mechanisms of action, and sums up the biomimetic super-hydrophobic design, the sacrificial type physicochemical characteristic. The article firstly classifies and introduces the functional types of coatings according to different mechanisms of action, and the latest research progress on the mechanism design of anti-icing coatings and their performance modification such as bionic superhydrophobic design, sacrificial physicochemical property design, microregion modulus control design and multifactorial coupling design were summarized. The problems of single-functionality and imbalance of performance of the existing coating mechanism design were analyzed and discussed, the view of the development trend and outlook of the development and application of icephobic coatings were put forward.

Keywords Functionally biomimetic, Superhydrophobicity, Design mechanism, Passive anti-icing, Icephobic coatings

*Correspondence:
Yuantao Zhao
zhaoyt@shmtu.edu.cn
Full list of author information is available at the end of the article

Springer

1 Introduction

Low-temperature freezing disasters are characterized by complex causes, high difficulty in prevention and response which cause extensive direct damage to energy and power, transportation, construction facilities and other important basic livelihood areas. Some studies have shown that icing increases flight resistance by 70% [1], increases the flight accident rate by 15% [2], reduces the efficiency of wind power by 80% [3] and reduces the efficiency of heat exchange by 20% [4]. And since the twenty-first century in the global economy active range expansion and extreme weather frequent co-edition, ice disasters have seriously affected the development of human society.

The anti-icing process can be divided into two phases, anti-icing and de-icing. De-icing is mainly when the icing behavior occurs on the surface of the object, the overlying ice on the surface can be effectively removed. Traditional methods include mechanical method, thermal method, chemical reagent method, ultrasonic guided wave method, etc., all of which are active de-icing methods with the help of external factor intervention, and there are many problems such as high energy consumption, low efficiency, destructive, limitation and heavy pollution [5, 6]. In particular, mechanical de-icing, which is still widely used in many scenarios such as aviation, wind power, transmission lines, etc., will bring permanent damage to the equipment and is not an ideal means of applying in actual production. In order to completely solve the occurrence of icing disasters, researchers, based on the theory of adhesion action to prevent icing, analyzed the physicochemical properties of the material and the surface structural properties and reduce the possibility of adhesion occurrence by reducing the three ideas of supercooled liquids on the surface of the object's hysteresis, contact area, and residence time [7], which is mainly achieved through the functional finishing and modification of the surface of the substrates Long-term "passive" prevention of icing is achieved mainly through functional finishing and modification of the substrate surface [8]. In addition, the ultra-low adhesion property of anti-icing/de-icing coatings also confers rapid autonomous de-icing characteristics with low energy consumption, high efficiency and low cost [9, 10]. Currently, physicochemical properties are used to prepare functional composite coatings using materials with properties such as low surface energy, storage and exchange of heat, and photoelectric heat. Surface structural properties are mainly constructed on the surface of the coating through the template method, chemical deposition, sol-gel method, laser etching and other processes to build a bionic three-dimensional micro-nano structures with superhydrophobic properties [11], and the use of supercooled water droplets and surface micro-nano structures in the process of contact with the media cavity capsule so that the liquid in the form of a large static contact angle (WCA) and a small rolling contact angle (WSA) to produce the "lotus leaf effect" [12]. For different design ideas, researchers have also carried out a large number of system design and development work, currently in the physical and chemical properties of the design with the development of basic materials science, the coating from relying on a single characteristic for the anti-icing performance of the shortcomings of the research tends to diversify the interactions of materials to generate force, such as in the low-surface-energy super-hydrophobic coatings on the basis of the integration of heat-producing characteristics of the material. In terms of surface structure design, with the development of processing technology, the coating structure tends to be more biomimetic, making full use of laser etching and other fine processing technology can be designed and constructed in the coating surface or internal more multilevel and complex structure.

The article categorizes anti-icing/deicing functional coatings into superhydrophobic coatings, sacrificial coatings, micro-area modulus coatings, and function-coupled coatings in terms of their mechanism and performance, summarizes the most recent research progress on the corresponding coatings, especially new methods and ideas for the design of coatings, and highlights their accomplishments, summarized the current state of research on the relevant coatings and its accomplishments, and examined the shortcomings and development trends of anti-icing/deicing coating technologies in order to serve as a guide for the investigation of future research directions on various coating types.

2 Bionic superhydrophobic design

The role of the ice layer on the surface of the object can be explained by the accumulation of ice adhesion mechanism, in which the static and dynamic adhesion is greatly influenced by the surface wettability of the accumulation of ice. The relevant theory is primarily mechanical, chemical bonding, and the liquid-like layer of a variety of mechanisms work together [13]. The primary methods of characterizing and establishing wettability are the WCA and WSA. According to the mechanism of interfacial wetting effect, hydrophobicity is classified into hydrophobic and superhydrophobic according to the solid-liquid interfacial contact state and angle, in which according to Young's proposed wetting state and equation for perfectly smooth surfaces, solid surfaces with WCA > 90° are considered to be hydrophobic and the surface is said to be superhydrophobic only when the WCA > 150° [14]. When a solid surface shows superhydrophilicity, water droplets in contact with the coated surface still maintain

a spheroid-like water droplet morphology, which is very easy to bounce or roll off, and therefore are not likely to adhere to the surface until the supercooled water solidifies. The nanoscale waxy layer and papillary micro-nano structures on the surface of lotus flower can achieve superhydrophobic performance from both low surface energy and micro-nano structures based on the principle of bionics. Table 1 summarises the study of biomimetic superhydrophobic surfaces prepared by different design methods.

2.1 Low surface energy coating and modification

Low surface energy coating refers to the introduction of organic or inorganic materials with low surface energy characteristics in polymer coatings, to obtain modified coatings that isolate oxygen atoms in water molecules, and to reduce the adhesion strength of the coatings, and the low surface energy materials currently used are mainly fluorine-containing and silicone modified polymers, which are also the two materials with the lowest known surface energy. The verdict was found that the surface energy of different groups in the order from high to low: $-CH_2 > -CH_3 > -CF_2 > -CF_3$, the lowest surface energy $-CH_2$ group (6.7mN/m) in the ideal smooth surface closely aligned to form the WCA extreme value of 120° [28], which is the upper limit of the WCA of a single smooth low-surface energy material [29].

Polytetrafluoroethylene (PTFE) was first synthesized by the American chemist Plunkett in 1938 with organofluoride polymers have a minimum surface energy of 18 mN/m, while polydimethylsiloxane (PDMS) first appeared in 1940 [30, 31], and organosilicon polymers have a minimum surface energy in the range of 20–30 mN/m [32], but due to the complex preparation conditions of PTFE, PDMS became the first choice for low surface energy coatings, driving the leapfrog development of low surface energy superhydrophobic polymer coatings. Numerous studies have shown that the silyloxy backbone of the silicone molecular chain in Fluorinated SiO_2 (F-SiO_2) NPs (NPs) surrounds the helical outward-facing methyl groups and have lower ice adhesion strengths than single fluorine-containing or silicone-based coatings [33]. Cao [15] prepared superhydrophobic F-SiO_2 anti-icing coatings by template method and chemical vapour deposition. The coated surface showed excellent repulsion of water and ice at low temperatures of -10 °C and about 85% relative humidity, and also exhibited good anti-icing and de-icing performance in dynamic and static tests. the very low ice adhesion strength of 14.8 kPa was reduced by 90% compared to the substrate. Crosslinking modification based on F-SiO_2 copolymer materials can further enhance the hydrophobicity and functionality of the coatings. Wu [16] prepared anti-icing coatings on diverse substrates through facile spraying the FSC/PDMS/ F-SiO_2 mixed solution with an artist's spray gun. Due to the specially designed chemical structure of FSC, silanol groups can be easily obtained via the hydrolysis of the chemically active methoxysilyl groups with slight moisture in the ambient environment (Fig. 1a). And negligible diameter variation of F-SiO_2 NPs, which

Table 1 Biomimetic superhydrophobic surfaces prepared with different design methods

| Design methods	Material	WCA	WSA	Adhesion strength	Literatura
Low surface energy coating and modification	F-SiO$_2$	-	-	14.8 kPa	[15]
	FSC15/PDMS/SiO2-F nanocomposite	160.4°	1.5°	56.7 kPa	[16]
	ZIF-7@ZnG@PFDS/EP superhydrophobic	164°	3.7°	-	[17]
	SiO2-FPU superhydrophobic	162°	2°	-	[18]
	Hierarchical PDMS NPs and PDMS MPs-P25	168.6°	3°	-	[19]
	Polydimethylsiloxane (PDMS) and cross-linked poly[hexeafluorobisphenol A-co-cyclotriphosphazene] microspheres (PHC)	164°	3.7°	-	[20]
	Polyurea ice-phobic coating (PUIC) developed from NCO-terminated pre-polymers, polyaspartate	125.3±1.6°	9.7°	23.7 kPa	[21]
Micro-nano rough structured surfaces	Polymer nanocone array coatings (NC)	156°	3°	-	[22]
	Polymer/graphene-based and F-SiO2 micro-nanoscale "radial" fiber network morphology	159.2°	4°	-	[23]
	Microblock structures and nanohair structures on aluminum substrates	162°	2±1°	-	[24]
	Micron cone + submicron flower + nanograss micro-nano structure superhydrophobic	161°	0.5°	1.45 kPa	[25]
	Fabricating microscale thin-walled lattice structures coated with a superhydrophobic layer	165.1°	-	-	[26]
	Rough microstructure with aluminum oxide particles; fluorosurfactant and fluorinated alkyl silane coating	>150°	<10°	-	[27]
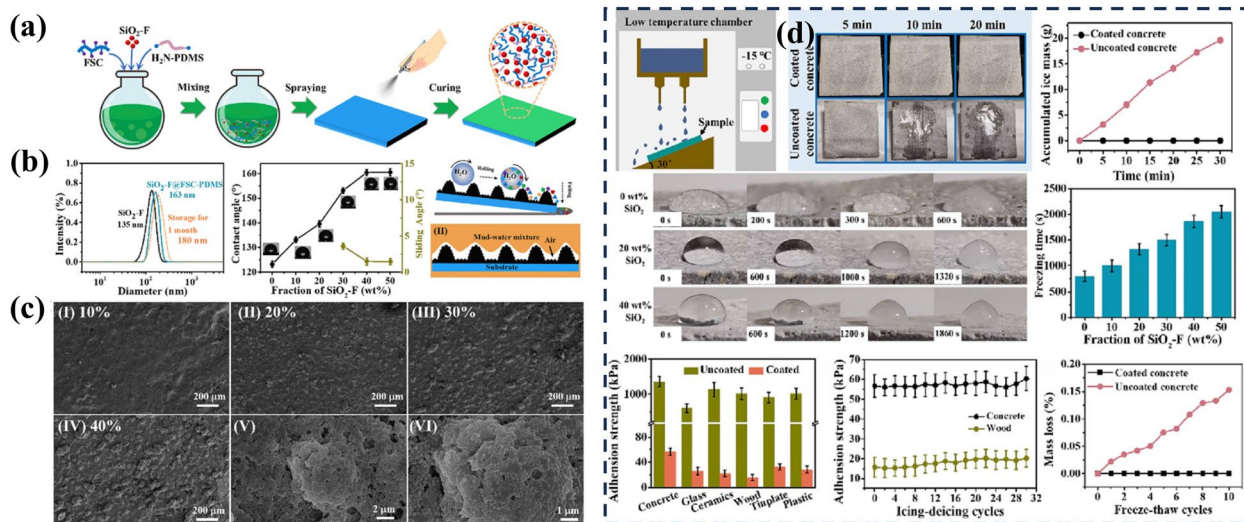
Fig. 1 The fabrication process of the FSC/PDMS/SiO$_2$-F composite coatings via spray-coating method; **b** Size distribution and variation of WCA and SA with different friction of SiO$_2$; **c** Schematic of self-cleaning (I) and anti-fouling (II) performances of the coating; **d** Anti-icing performance of FSC/PDMS/SiO$_2$-F composite coating [16]

guarantees the potential of long-term storage and long-distance transportation in practical application with WCA = 160.4° and WSA = 1.5° (Fig. 1b). the surface is relatively smooth at 10 wt% F-SiO$_2$ NPs loading. As the F-SiO$_2$ NPs content increased, the surface morphology of the coating became rougher and an increasing number of microscale bulges were observed at low magnification (Fig. 1c). the anti-icing coatings prepared at -15 °C can delay the freezing time up to 1860s (Fig. 1d).

Low surface energy organic coated polymer chains usually have poor mechanical wear properties and ensure long-lasting performance in complex and variable environments is difficult. The coatings can be made mechanically wear-resistant and self-repairing by introducing inorganic wear-resistant materials or grafting modification. Zhu [17] synthesized ZIF-7@ZnG NPs with zinc gluconate and modified them with 1H,1H,2H,2H-perfluorododecyltriethoxysilane (PFDS) which epoxy resin (EP) as the connecting layer was introduced to prepare ZIF-7@ZnG@PFDS/EP superhydrophobic coatings (Fig. 2a). WCA = 164°, WSA = 3.7° with self-healing properties. Fu [18] synthesized mechanically robust SiO$_2$-FPU superhydrophobic coatings on a variety of substrates by a two-step thiol click reaction. Branched fluoroalkyl chains were grafted onto the polyurethane backbone and the flexible fluoroalkyl chains tended to migrate to the surface while the strong urethane bonds were located on the substrate. The flexible and branched fluoroalkyl chains accelerate the migration to the surface of the coating when heated and rebuild the nanoscale structure conferring self-healing properties (Fig. 2b).

The low light transmittance, poor mechanical strength and unsatisfactory chemical stability of superhydrophobic coatings greatly limit their practical applications. Zhu [19] proposed a hierarchical coating (P25) consisting of PDMS NPs and PDMS particles (MPs) functional NPs, and the photoresponsive properties of P25 could be achieved by repeated UV irradiation and dark environment storage to achieve reversible wettability between superhydrophobicity and hydrophobicity. The superhydrophobicity and high light transmittance of more than 76% were maintained after mechanical impact. Hong [20] crosslinked and polymerized PDMS with [hexafluoro-bisphenol-A-co-cyclotriphosphonitrile] microspheres (PHC) (Fig. 2c) with the coatings exhibited superhydrophobicity (WCA = 164°, WSA = 3.7°). The coating exhibits exceptional mechanical durability against various damages due to the synergistic effect of the micro-nano structure surface and the strong and stable interaction between the PHC particles and PDMS.

Nevertheless, low ice adhesion strength is frequently unattainable for stiff materials with high elastic elasticity. The self-healing capacity at below-freezing temperatures is difficult to replicate for manufactured icephobic surfaces, and is frequently unaffordable. When combining various components to create icephobic materials, the varying moduli of the materials could lead to an uneven distribution and phase separation. Li [21] has revolutionised ice-phobicity and robustness by using a combination of soft and hard segments impregnated with lubricants. Based on this strategy, a polyurea ice-phobic coating (PUIC) developed from NCO-terminated prepolymers,
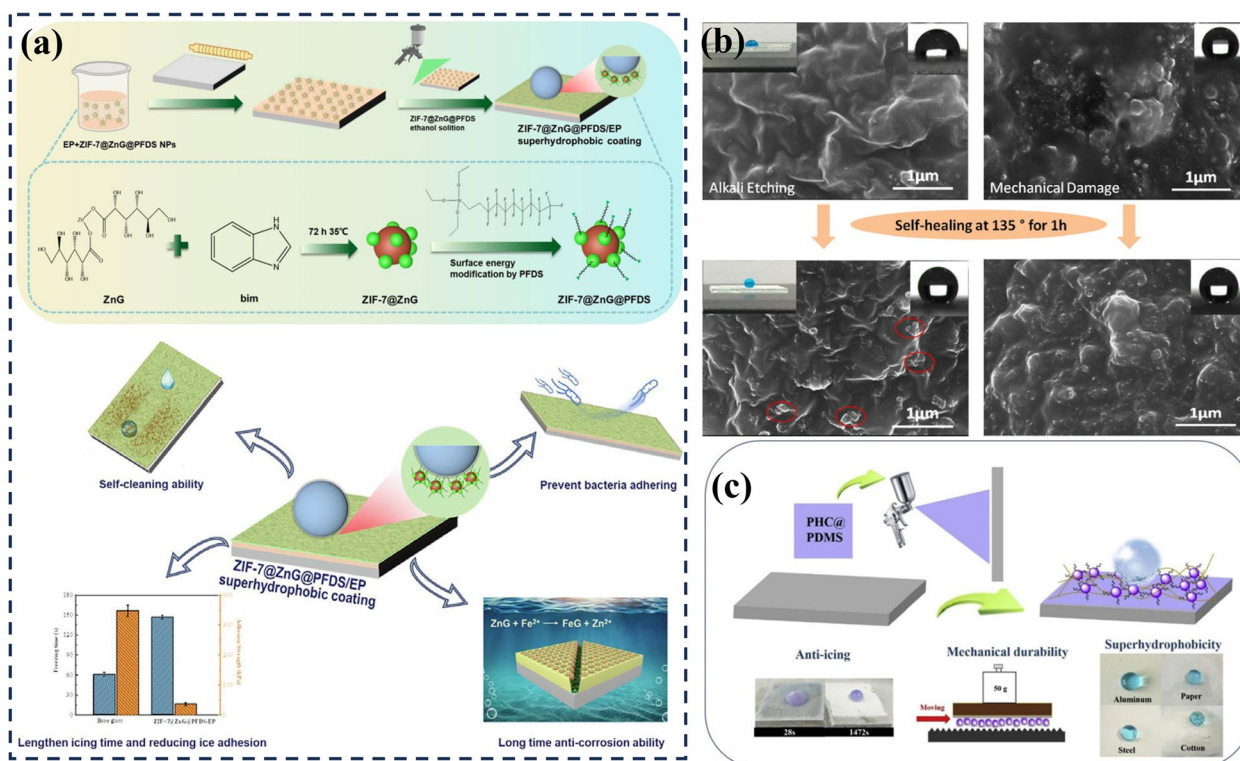
Fig. 2 a Preparation process of ZIF-7@ZnG nanoparticle (NP) modified PFDS superhydrophobic coating synthesized with zinc gluconate and its anti-icing properties [17]; **b** Self-healing effect of coatings 1 h after mechanical abrasion [18]; **c** Mechanical strengthening of PDMS surfaces by PHC particle micro-nano structures [20]

polyaspartate, and dimethicone oils ensured fast and non-destructive ice detachment at the interface by the synergistic action of hydrophobicity, elastic deformation, and interfacial sliding (WCA ~ 125.3 ± 1.6°, WSA ~ 9.7°, low ice adhesion strength ~ 23.7 kPa). In addition, the resulting PUIC not only withstands 5000 consecutive Taber abrasion cycles before the coating is completely worn out, but also remains ice-repellent under 50 icing/de-icing cycles, 72 h of acid/alkali immersion, 72 h of UV radiation, and 240 h of neutral salt spray conditions. Additionally, damaged PUICs can be recovered with organic solvents and maintain good ice repellency. PUICs are ice-repellent, robust, and scalable, making them effective for static mass de-icing and dynamic anti-icing, and have great potential for practical applications.

2.2 Micro-nano rough structured surfaces

The judgement condition of the interfacial contact angle theory proposed based on Young's wetting equation is an ideal absolutely smooth plane, but solid surfaces in practical application scenarios are bound to have the presence of roughness [34]. The proposal of Wenzel's wetting equation elucidates the basic relationship between roughness and contact angle, i.e., the larger the roughness, the larger

the contact angle of hydrophobic surfaces is approximately, indicating that building surface roughness structure is an important way to regulate surface wettability [35]. However, the "lotus leaf effect" exists in nature with more complex interfacial states, and the Cassie-Baxter equation better explains the superhydrophobic behavior based on the special composite contact interface, which suggests that the droplets cannot fully penetrate and fit on the roughness surface, and more microstructures are needed to form air cavities (Fig. 3), i.e. increasing the proportion of air cavities per unit contact area [36]. Barghi [37] further demonstrated that the Cassie-Baxter model microconvex body transforms the interfacial contact phase by trapping the gaseous phase, weakening the direct interaction with the droplet, resulting in a reduction of the energy barrier to be overcome for the droplet motion.

In recent years, there have been new attempts in micro-nano rough structure preparation processes to further enhance the density and uniformity of the structures. Anvesh Gaddam [38], Guo [39], Zheng [40] and Wang [41] constructed superhydrophobic surfaces with periodic micro-nano structures by femtosecond laser on stainless steel, copper substrate, titanium alloy and
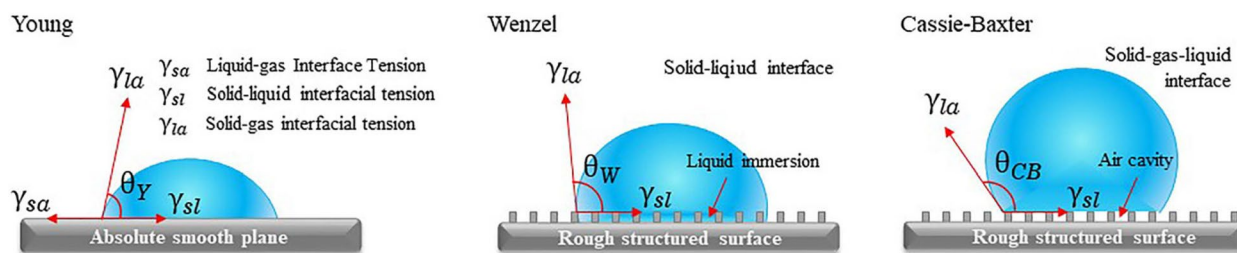
Fig. 3 Schematic of Young, Wenzel and Cassie-Baxter models of surface wetting theory

aluminum alloy surfaces, respectively, obtaining surfaces with WCAs all exceeding 165° and sliding angles as low as 1.2°. Zhang [42] used a direct network embossing method and a layer-by-layer assembling technique on fluorocarbon varnish coatings for innovatively constructed modified silica NPs superhydrophobic coating with a large-area micropillar array structure. The process further reduces the width of the micropillars to increase the density of microgrooves, forming a stronger air cushion effect and delaying the penetration of corrosive media.

In addition to the conventional micropillar array structure, researchers are also developing other forms of micro-nano structures to seek for more efficient superhydrophobic effects. Huang [22] found that regular polymer nanocones coatings (NCs) arranged vertically can be obtained by the newly designed iCVD process using cohesive nano-sized monomer droplets as the nucleation centre, and relying on the adjusted deposition conditions to effectively control the height and density of the nanocones, and the hydrophobicity and light transmittance of NC was 2.2 times higher than that of the coating with an irregular surface microstructure. Chen [43] proposed an innovative combination of a macroscopic aluminum honeycomb structure with a superhydrophobic coating, which, compared to common superhydrophobic coatings, resulted in the reduction of the heat transfer between the macroscopic honeycomb wall and droplets due to the reduction of the heat transfer between the single droplets on a the surface at -15 °C extended the summary ice time by 190 s. After 300 wear tests, the amount of frost formation increased by only 0.03 g after tilting by 60% (-20 °C, 75 ± 5%wt). Ge [44] femtosecond laser on polytetrafluoroethylene (PTFE) substrate Two novel structures, Siberian-Cocklebur-like microstructure and square column integrated Siberian Cocklebur-like microstructure, were prepared, and the microscopic morphology and properties (Fig. 4). Compared with the traditional structure, the new structure has a larger water contact angle in the low-temperature environment, which can effectively inhibit the vapour condensation in the microstructure and improve the anti-icing performance of PTFE surface in the low-temperature environment. Zheng [23]

combined polymer/graphene-based and F-SiO$_2$ materials to construct a micro-nanoscale "radial" fiber network morphology, and the WCA and WSA of the prepared coatings reached 15% and 15%, respectively, when the graphene content was 6 mg/ml. At a graphene content of 6 mg/mL, the WCA and WSA of the prepared coatings reached 159.2° and 4°. Respectively, the lamellar structure of graphene and the internal fiber network morphology endowed the coatings with robust mechanical durability.

The droplet diameters in nature are broad and random make a single micro-nano structure cannot completely guarantee superhydrophobicity for droplets of all sizes. The droplet diameters in nature are broad and random, and a single micro- and nanostructure cannot fully guarantee superhydrophobicity for all sizes of droplets, and the established Cassie-Baxter equilibrium state can be easily broken. Guo [45] firstly discovered that multilevel micro-nanostructures can effectively provide a more stable Cassie-Baxter equilibrium state through a comparative study of hierarchically structured ice-sparing surfaces, individually micrometre-structured surfaces, ZnO nanorod-structured surfaces and smooth surfaces. In the process of condensation and icing, water droplets absorb heat from the air in the form of contact heat conduction and heat radiation, while heat is dissipated to the cold surface through contact heat conduction and heat radiation between droplets and nanobristles surface, which is a system of solid-liquid-air three-phase interface. Since the liquid-solid contact area on the surface of micro-nano structures surface is small and the percentage of air trapped between the micro-gaps on the surface is high, the heat loss through contact heat conduction is small. Moreover, the nanomaterials can effectively prevent the gas-liquid interfacial slip induced by the Laplace pressure, so that the whole system is in a constrained Cassie-Baxter equilibrium. In recent years. Shen [24] demonstrated that when a large number of supercooled droplets with diameters of 20–40 µm hit the micro-structured superhydrophobic surfaces, their anti-icing performance was lower than that of the nanostructured superhydrophobic surfaces, which indicates that the anti-icing performance of the structure is still
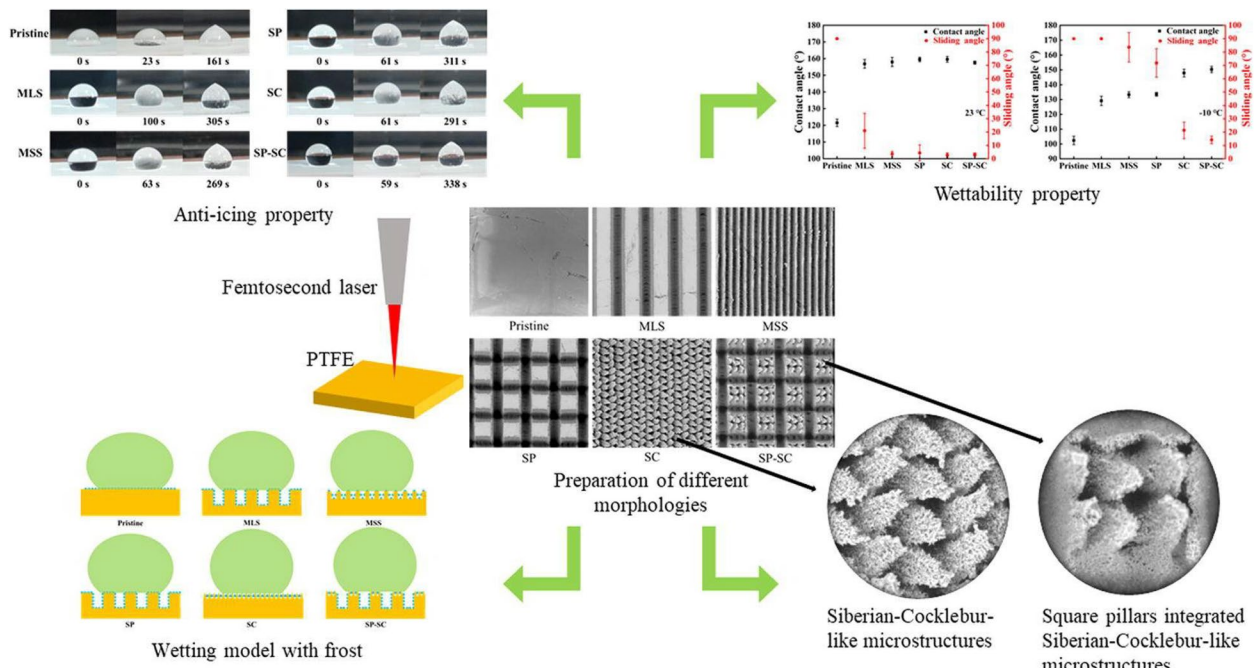
Fig. 4 Micromorphology and hydrophobic properties of Cocklebur and Cocglebur Siberian-like structures constructed on PTFE surfaces [44]

varied depending on the This indicates that the anti-icing performance of the structures is still different depending on the size. The establishment of multilevel micro-nano structures with size gradient can enhance the stability and applicability of superhydrophobicity. Currently,

Tsinghua University constructed a new three-stage micro-nano structured superhydrophobic surface of "micron cone + submicron flower + nanograss" through a synergistic process of laser ablation and chemical oxidation (Fig. 5a) [25]. Under the high humidity condensation

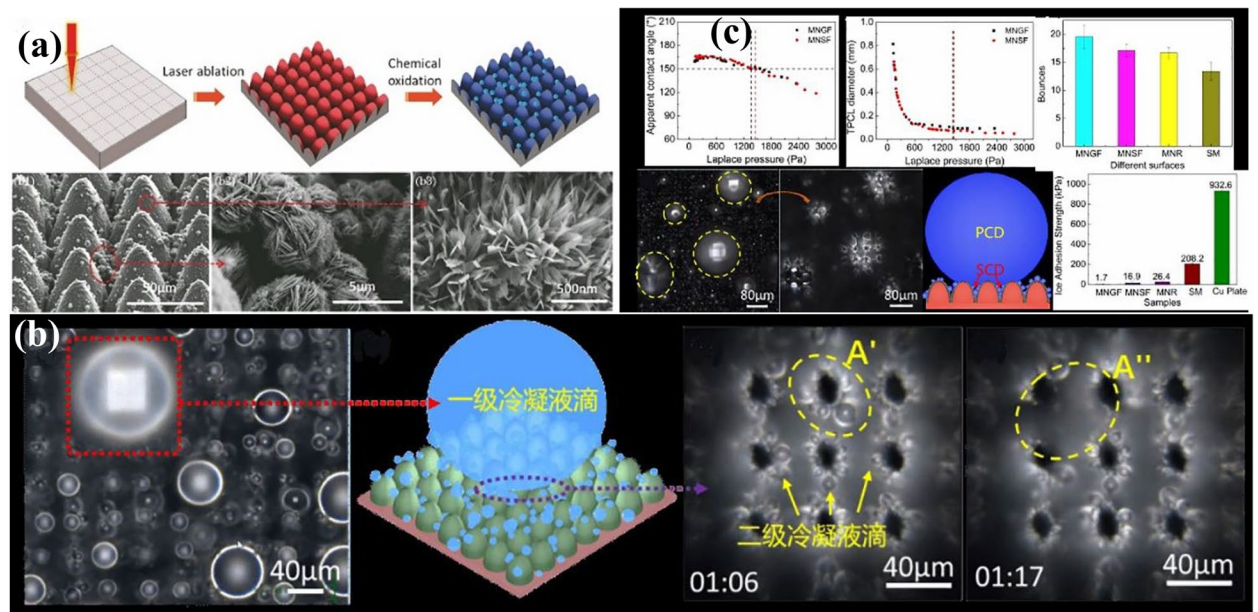**Fig. 5** **a** Microstructures of tertiary micro-nano-superhydrophobic surfaces prepared by ultrafast laser composite method; **b** Graded condensation and merging of condensed droplets on a tertiary micro- and nanoscale superhydrophobic surface induces self-jumping phenomena; **c** Characterization of Cassie state stability and anti-deglaciation properties of a tertiary micro-nanoscale superhydrophobic surface [25]

environment, the surface undergoes graded condensation and the merging-induced self-jumping phenomenon of condensed droplets (Fig. 5b), and the condensed secondary droplets in the tertiary micro-nano structures are continuously merged into the primary condensed droplets on the surface, so that the primary droplets continue to have a better stability of Cassie's state with a WSA of up to 161°, while the WCA of only 0.5°, and a critical Laplace pressure of up to 1450 Pa, which has been reported to be the highest in the world, with a WSA of up to 161° and a WCA of only 0.5° (Fig. 5c). The critical Laplace pressure is up to 1450 Pa, which is the highest stability superhydrophobic surface reported, and ice can be shed by self-gravity. Multi-stage micro-nano-structures can also reduce the damage of large droplets on surface properties during droplet condensation through droplet screening. Ma [26] utilized the large tolerance of aggregation mismatch for jumping as well as the effective isolation mechanism of droplets between neighbored lattices to realize the condensation droplet screening through the microsized thin-walled lattice structure constructed on the surface of superhydrophobic layer and the droplets growing a little bigger than the lattice size bounced from the surface. surface bouncing. The maximum radius and residual volume of the droplets can be strictly limited to 16 μm and 3.2 nl/mm^2 by designing the dimensions of the micro-nano structures respectively.

Superhydrophobic surfaces are currently the most widely researched and applied anti-icing strategy, but the current superhydrophobic coatings, although with excellent superhydrophobic anti-icing performance, have problems such as poor resistance to mechanical abrasion and chemical corrosion due to structural peculiarities, which seriously limit the application prospects of such coatings. Self-healing superhydrophobic coatings with self-healing ability can effectively alleviate this problem. The main mechanism of self-healing coatings is to make use of their own physical and chemical properties, under the stimulation of certain external factors such as light and heat, the activation of accelerated energy occurs in response to some of the reversible chemical bonding of the polymer to complete the self-bonding, which greatly reduces the time required for healing. On the other hand, healing agents are carried to repair the damage by external introduction of healing agents such as microcapsules, hollow-core fiber coating and construction of capillary system [27]. According to Zhang [46], a novel idea and environmentally benign technique based on a waterborne solution may be used to create long-lasting superhydrophobic and oleophobic surfaces with the ability to cure themselves. In this idea, fluorosurfactant and fluorinated alkyl silane were used as low surface energy materials, while aluminum oxide particles were used to provide the rough microstructure (Fig. 6a). With a water contact angle more than 150° and a sliding angle lower than 10°, the surface demonstrated good water repellent ability. By using the special chemical makeup and microstructure of layered double hydroxide (LDH) material, Liu [47] created an aluminum alloy 6061 superhydrophobic Ni-Al LDH coating with self-healing capabilities by hydrothermal reaction and low energy modification. Investigations were done into how hydrothermal factors affected the coating's microstructure and wettability. The nanowall array-prepared coating shown exceptional superhydrophobicity with contact angles of 162.1° and 1.9°, respectively (Fig. 6b). The coatings demonstrated strong resistance to a variety of hard conditions and fast self-healing after losing their superhydrophobicity.

Although the current self-healing coatings can improve this problem, there is still a lot of room for improvement in self-healing performance, and the related preparation process is complicated and time-consuming, chemical contamination of raw materials, and the healing efficiency and uniformity are not high. So there is a need for a simple, green, and long-lasting design and preparation technology, which can reduce the conditions of the superhydrophobic coating in the large-scale application of the limitations. At the same time, in the North and South Polar regions and other extreme ultra-low temperature (below -50 ℃) conditions, supercooled water is Wenzel adhesion state when the anti-icing effect is greatly reduced, once the icing of the micro-nano structures, but the formation of mechanical interlocking effect is very difficult to remove, even if the removal of the surface structure of the mechanical damage caused by a large area of ultra-thick ice-covered solution to the problem of difficulty.

3 Design of sacrificial physicochemical properties

Sacrificial coatings, on the other hand, refers to the inhibition of the nucleation growth or retention of supercooled water and ice crystals through the release of chemical mediators such as small molecules and lubricating fluids with certain physicochemical properties [29]. At present, according to the icing mechanism and process, the more appropriate chemical media action mainly include two mechanism: (1) rely on molecular intercalation to actively reduce the condensation point of water molecules, inhibit the nucleation process of supercooled water; (2) rely on the release of low-surface-energy lubricant to form a super-lubricating isolation medium membrane can reduce the strength of the surface adhesion, and at the same time to improve the nucleation barriers to inhibit the icing. Table 2 summarises the study of sacrificial physicochemical properties coatings prepared by different design methods.
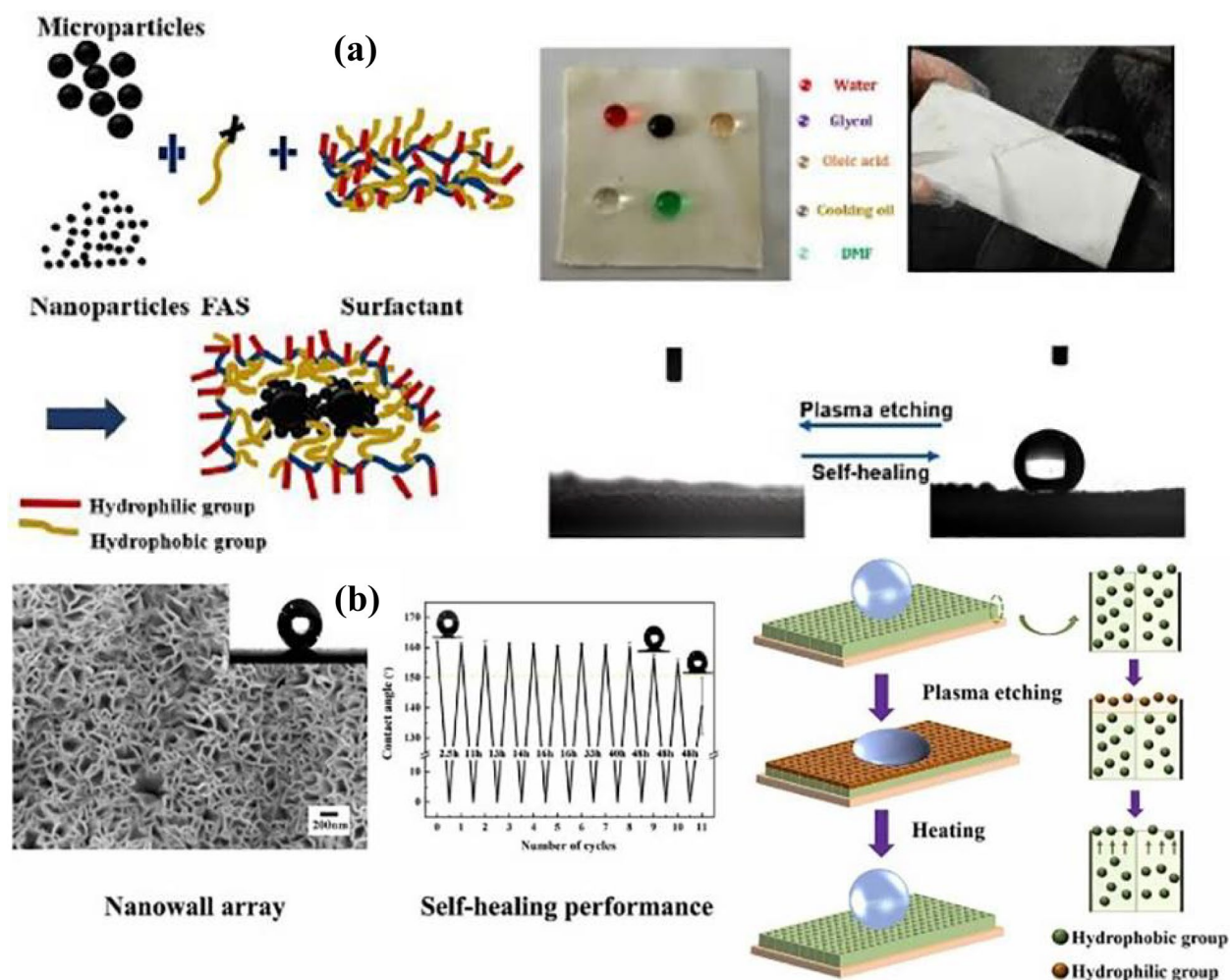
Fig. 6 a FAS and fluorosurfactant forming biphobic interaction, plasma etching forming self-healing surface [46]; **b** Ni-Al LDH forming microscopic nanopore array structure, showing excellent superhydrophobicity with contact angle of 162.1±0.4°, hydrothermal reaction of self-healing process [47]

Table 2 Sacrificial physicochemical properties coatings prepared by different design methods

Design methods	Material	WCA	WSA	Adhesion strength	Literatura
SLIPS	Different morphologies with NPs of different sizes and shapes, coatings with bistable (i.e., superhydrophobic and slippery) states	152.4±5°	6±1°	2.5kPa	[48]
	Superhydrophobic fluorinated chain segments with hydrophilic hydroxyl and amino groups	106°	3°	-	[49]
	The porous framework consisted of polydimethylsiloxane (PDMS) and softener, and inert dimethyl silicone oil	>110°	20°	15 kPa	[50]

3.1 Liquid-containing lubrication of porous surfaces

In 2011, Aizenberg of Harvard University developed a liquid-lubricated porous bionic surface, also known as liquid-infused porous superslip surface (SLIPS), inspired by the surface lubrication mechanism of Porcupine [51]

(Fig. 7a). SLIPS is based on the construction of interconnected interpenetrating micro-nano hierarchical porous structures on the surfaces of superhydrophobic materials, and a low surface energy lubricating liquid with water repellency is immersed and locked on the surface
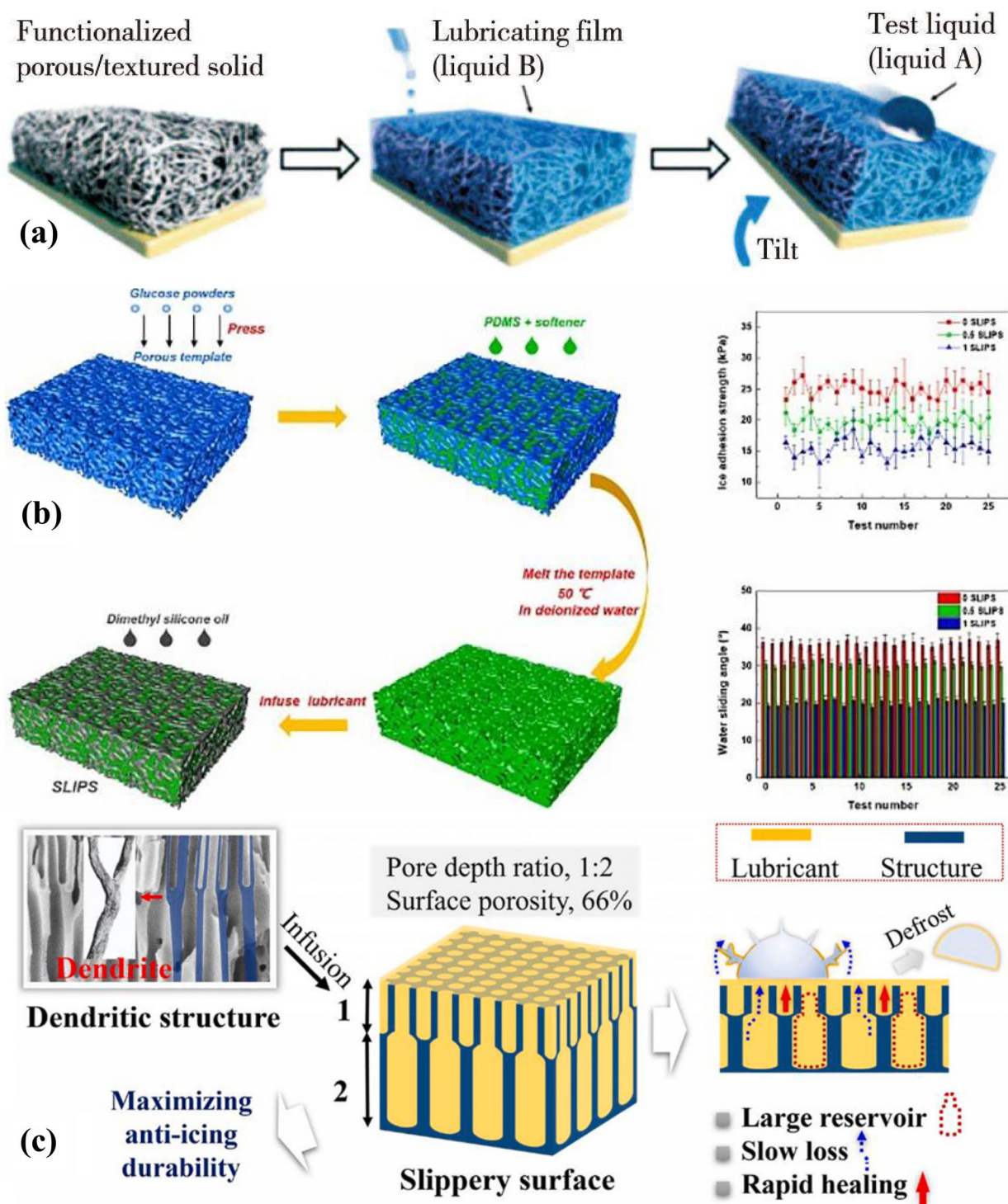
Fig. 7 a Schematic diagram of SLIPS coated porous bionic structure with liquid lubrication [51]; **b** Bistable transition mechanism and hydrophobic properties of SLIPS-modified surfaces [50]; **c** Y-SLIPS Coating internal structure and oil locking mechanism [53]

of the surface. energy lubricating liquid with hydrophobicity is immersed and locked in the porous matrix. The contact of supercooled water with the surface can

effectively inhibit the adhesion and reduce the nucleation temperature due to the mutual repulsion and slip of the superlubricating interface, which also helps to improve

the mechanical stability of the superhydrophobic coatings [52]. Li [48] proposed a new type of multifunctional SLPIS coatings, where the relationship between superhydrophobicity and lubricity was established. The clever adaptive conversion mechanism between superhydrophobicity and lubricity where superhydrophobic coatings with different morphologies were prepared using NPs of different sizes and shapes, and coatings with bistable (i.e., superhydrophobic and slippery) states were obtained by injecting dodecane, where both the superhydrophobic and smooth surfaces could effectively drive the movement of supercooled water and retard condensation crystallization.

The biggest problem of SLPIS coatings at this stage is that the lubricating medium itself will continue to deplete due to gravity, external impact and other behaviors resulting in limited lifetime, and researchers are also trying to improve the self-replenishing or oil-locking ability of the coatings. Li [49] constructed SLIPS with spontaneous micro-phase separation by a stepwise deposition strategy, and the superhydrophobic fluorinated chain segments with hydrophilic hydroxyls and amines with a The significant polarity difference between the superhydrophobic fluorinated chain segments and the hydrophilic hydroxyl and amino groups caused the coating to produce spontaneous microphase separation on the surface, achieving ultra-stable oil locking capability. Organic lubricants are generally stored between the organic polymer chains of elastomers and the micro-pressure given by water droplets, etc. prompts the deformation of elastomers in the dissolved state, and the gradual release of organic lubricants makes up for the loss of lubricants in the de-icing process, and this unique self-replenishing mechanism enables organic lubrication of anti-icing surfaces to improve durability. Qian [50]. This study prepared the slippery lubricant-infused porous surface (SLIPS) using an easy-to-use template method. Polydimethylsiloxane (PDMS) and softener made up the porous framework, and inert dimethyl silicone oil was poured into the pores to act as a lubricant. The sample was easily compressed under low external pressure, which caused silicone oil to extrude to the sample surface and increase surface lubrication. The silicone oil was kept inside the SLIPS when there was no pressure. This characteristic that responds to pressure prevented both rapid lubricant loss and prolonged exposure. The softener's composition was changed to fine-tune the pressure-responsive characteristic (Fig. 7b). when under external pressure or magnetic field, the lubricant stored within the coating will be released to the surface in a staged retardation, and after 25 icing/de-icing cycles, the ice adhesion strength on the surface is still below 20 kPa. Xiang [53] created a dendritic porous structure while taking the lubricant's

"storage-depletion-healing" into account. The pore depth ratio and surface porosity were then tuned. Furthermore, an investigation was conducted into the anti-icing durability of the dendritic slippery surface, or Y-SLIPS (Fig. 7c). The findings indicate that 66% surface porosity and a 1:2 upper-to-lower pore depth ratio are the ideal values, respectively. In an environment with frost and ice, the Y-SLIPS exhibits superior anti-icing durability in contrast to the conventional slippery surface (I-SLIPS). At the 140th frosting/defrosting cycle, the Y-SLIPS surpasses 20 kPa, but the I-SLIPS achieves this level at the 100th cycle. Rykaczewski [54] inspired by the functional and bilayered structure of poison dart frog skin, a stimuli-responsive antifreeze-secreting antifreeze coating was prepared, which consists of an outer epidermis with superhydrophobic pores and an inner epidermis with an antifreeze-injected core that slows down antifreeze release.

The traditional SLIPS preparation process is cumbersome, and the common method of substrate structure construction has a small applicable area and strict requirements on the substrate material, which hinders the large-scale application of SLIPS coatings. Starting from the underlying logic of SLIPS construction, the team from Sun Yat-sen University proposed the concept of "endogenous" SLIPS coatings, thus changing the idea of "filling liquid lubricants into solid structures" to "growing solid structures in situ from liquid lubricants" [55]. The concept of "endogenous" SLIPS coatings transforms the idea of "injecting liquid lubricants into solid structures" to "growing solid structures in situ from liquid lubricants", and enables SLIPS coatings to be formed through a coating-curing process just like ordinary commercial coatings (Fig. 8a). Based on this concept, the team has cleverly applied the classic Thermal Induced Phase Separation (TIPS) method of porous film preparation to the one-step construction of SLIPS, which requires the polymer and diluent to form a homogeneous solution at high temperatures, and then split into phases to form a solid-liquid composite structure at low temperatures. Conventional silicone oil-based lubricants are difficult to dissolve the polymer, so a third component was added to the system as a co-solvent to develop a polypropylene/silicone/hexadecane ternary phase separation system. After the low-temperature phase separation process, a network structure is formed inside the coating consisting of microscopic spheres connected together, and the lubricant is retained in the network by capillary action (Fig. 8b). The resulting SLIPS coating not only has good lubrication effect, but also has better long-term stability than the same coating obtained by the post-infusion
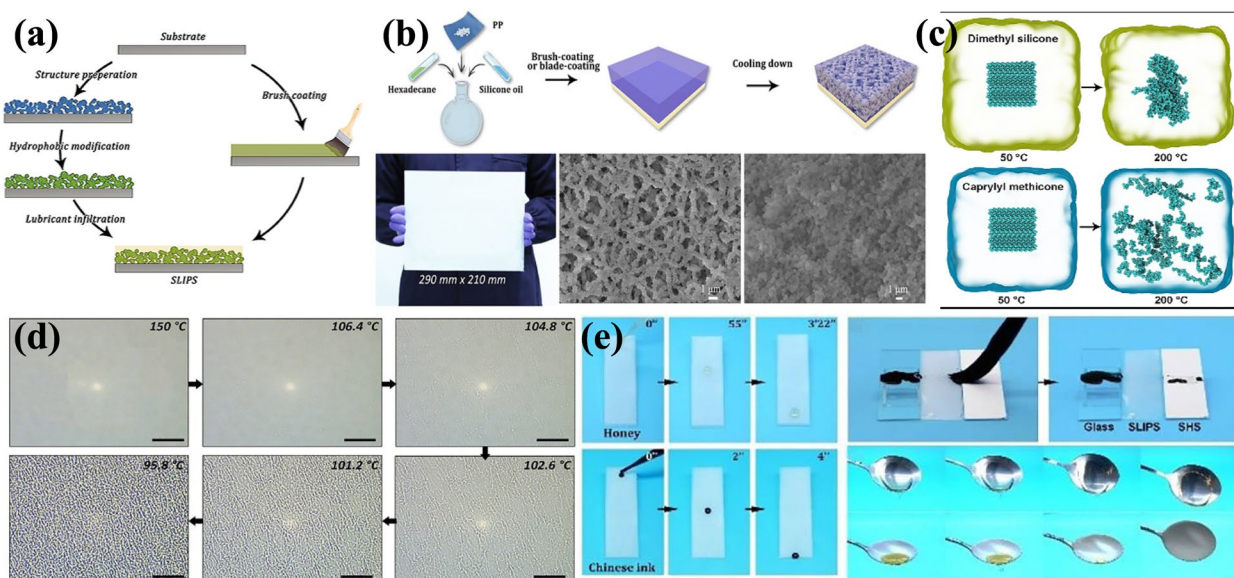
Fig. 8 Design and performance of "endogenous" SLIPS structures: **a** Reverse Preparation Route for SLIPS Structures [55]; **b** Schematic of one-step preparation of SLIPS coatings constructed by ternary split-phase system and macro/micro morphology of the coatings [55]; **c** Molecular dynamics simulation of polypropylene dissolution behavior in dimethicone and octyl silicone oils [56]; **d** Microscopic phase separation processes between polymers and lubricants in coating systems [56]; **e** Hydrophobicity and anti-adhesion properties of SLIPS coatings [56]

method because the solvent adapts well to the pore structure during the formation process. However, it was found that the ternary system is not only more complex, with more variables that are difficult to control, but also has a high cetane freezing point (18.2 ℃), making it difficult to use at low temperatures. In order to reduce the complexity of the reaction system, on the basis of the previous research, the "solubilizing group" and "lubricating group" were combined on the same molecule, combined with the means of molecular dynamics simulation, and the octyl silicone oil/ polypropylene system was selected as the coating construction material [56] (Fig. 8c). The results of molecular dynamics simulations show that the octyl group acts as a "diluent" and interacts with the polypropylene to promote its dissolution, while the silicone group regulates the compatibility of the system, allowing it to split into phases at low temperatures, and also acts as the main component of the lubricant. During the cooling process, it is obvious that the polymer nucleates from the system with the decrease of temperature and finally forms a particle network, and it can be concluded that the system has gone through the liquid-liquid split-phase and liquid-solid split-phase phases by combining with DSC and other means (Fig. 8d). SLIPS coatings exhibit excellent lubrication properties, showing good anti-adhesion to different liquids and even high viscosity honey. At the same time, the coating has excellent

ice adhesion resistance down to 1.9 ± 0.4 kPa (Fig. 8e), which is promising for anti-icing applications.

3.2 Chemical slow-release antifreeze coatings

Unlike SLIPS technology that requires surface structure, chemical slow-release coatings rely on the preparation process to embed sol systems, antifreeze, gels and other materials into ordinary coatings to obtain modified anti-icing coatings, where the materials slow or even inhibit the ice crystal nucleation process in the state of supercooled water by releasing chemical molecules with lower freezing point to reduce the freezing temperature of the supercooled water. He [57] firstly achieved the triple regulation of nucleation suppression, thermal conductivity reduction and low adhesion is realized. The hydrophobic polydimethylsiloxane links are branched in the hydrophilic polyelectrolyte network, and the polyelectrolyte hydrogel is obtained after advantageous integration, which regulates the nature of interfacial water through the synergistic effect of hydrophobicity and ionic specificity (Fig. 9a), so that the polyelectrolyte hydrogel coating is effectively and slowly released, and the ice nucleation temperature is lower than -30 ℃, the ice expansion rate is lower than 0.002 cm²/s, and the ice adhesion strength is lower than 20kPa. Li [58] proposed a sustainable self-deicing surface based on an ion diffusion mechanism, which inhibits water droplets from freezing for more than 5 days, reduces the adhesion strength to the Pa level, and tilts the surface to slide off automatically.
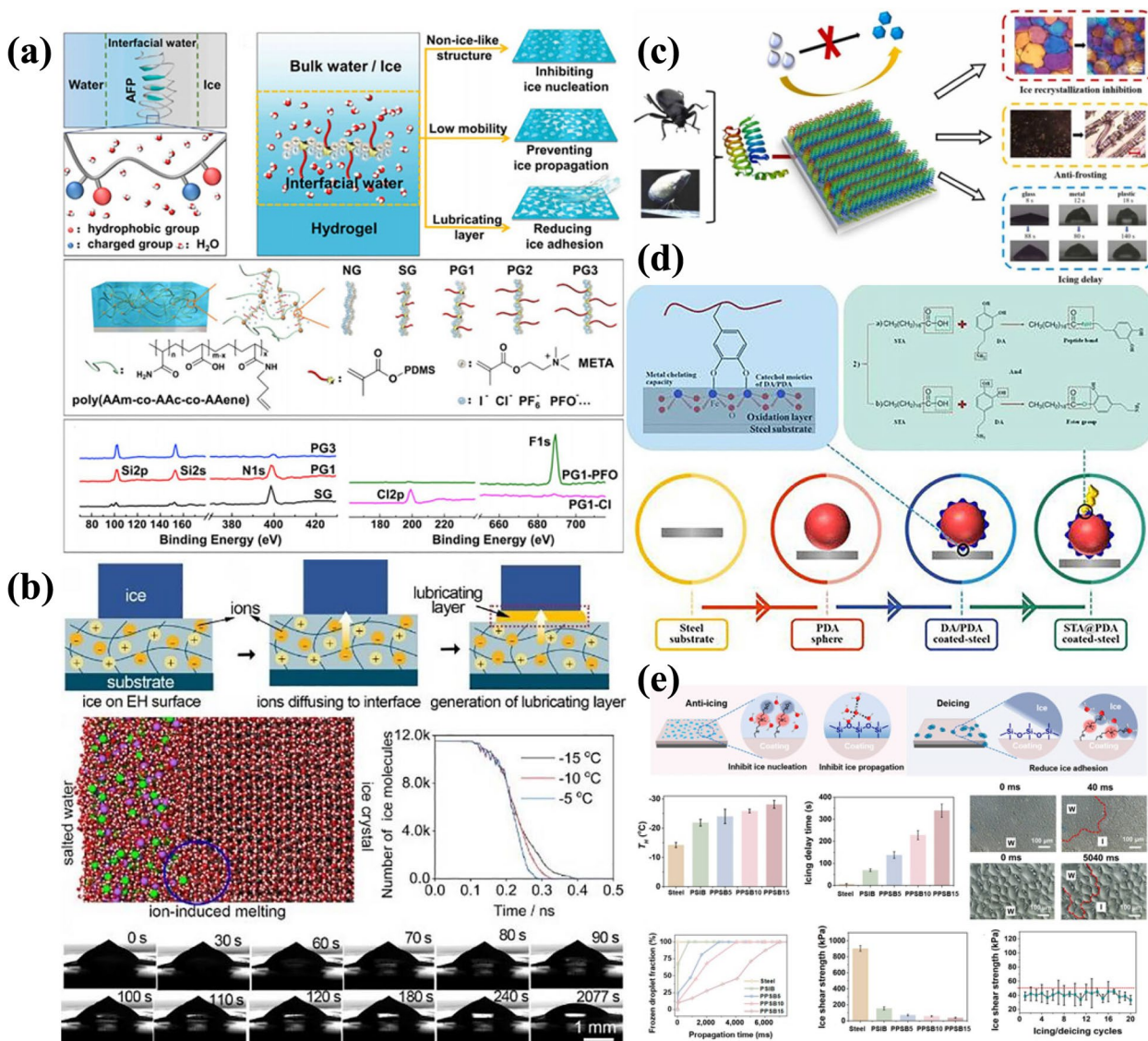
Fig. 9 **a** Bioinspired Design of Multifunctional Anti-icing Hydrogel Surfaces [57]; **b** Self-generation mechanism and nucleation inhibition effect of EH surface lubrication layer [58]; **c** Surface immobilization mode of insect antifreeze proteins and their anti-icing properties [59]; **d** Due to metal chelating ability between polydopamine catechol fraction and steel [60]; **e** Anti-icing mechanism and performance of bionic self-healing anti-icing coatings [61]

The anti-icing system can be regulated up to -48.4 °C by modulating the ion type and concentration. Molecular dynamics (MD) simulations and in situ experimental studies showed that the continuous diffusion of ions into the ice-material interface led to the continuous melting of ice crystals (Fig. 9b).

The mechanism of action of sacrificial coatings relies heavily on the release of chemicals, and chemically synthesized antifreeze can be contaminated by droplet adhesion into the atmosphere or soil environment. In nature, many animals such as arthropod crustaceans,

especially marine organisms within the North and South Polar seas, can tolerate extreme cold, mainly because organisms protect critical lethal cells from freezing through the combined action of their own internal body production of a protein with the ability to limit supercooling and induce freezing, the protein ice-nucleating agent (PIN), and cold-tolerant protein (ATP) [59]. Therefore, researchers have verified the feasibility of physiological cold-tolerance properties of organisms in special environments for biomimetic applications in industrial ice protection. Gao [59] and

Tian [60] combined an adhesion structural domain of mussel origin with the structural domain of antifreeze proteins derived from the yellow mealworm to obtain the chimeric protein multifunctional Mfp-AFP. Beetle-derived antifreeze fragments could resist frosting and delay freezing (Fig. 9c), and the chimeric protein containing the adhesion structural domain of dopamine also conferred non-selectivity of the coating towards the substrate (Fig. 9d).

Inevitably, anti-icing coatings are subject to mechanical damage during service, and the formation of 'wounds' that fail can make de-icing more difficult. Inspired by the self-healing "wounds" of biological tissues, endowing anti-icing coatings with self-healing ability can mitigate the effects of damage. Shu [61] found the NIBS-mimicking module and amphiphilic ionic chain segments of PDSB bind water molecules separately to reduce the heterogeneous nucleation temperature to -29.4 °C and the ice adhesion strength to 38.9 kPa. Meanwhile, the self-healing of the mechanical, anti-icing, and deicing properties of PDSB at -20 °C is achieved through the multi-dynamic bonding of the molecular structure with the strong hydrogen bonding, weak hydrogen bonding, disulfide bonding, and electrostatic interactions. and de-icing properties at -20 °C (Fig. 9e).

Sacrificial coating in service in the process of filling the chemical medium due to their own gravity, adhesion, etc. inevitably produce viscosity loss, although there have been relevant research for the inhibition of chemical medium loss, but the locking oil self-repairing ability can not ensure that the coating's longevity, resulting in the performance of the performance of the attenuation or even failure to seriously limit its potential for application and the existence of the preparation of high-cost, process complexity, poor weathering stability and other issues.

4 Microregion modulus control design

The interface state that exists during the contact process between the liquid droplets and the coating surface is one of the influencing factors for the formation of ice crystals from the condensation of supercooled water and its removal process. According to the theory of material mechanics of the interface, in the presence of modulus differences in the ice-coated coating when applying external forces, the ice first in the smaller modulus of the interface at the shedding of the formation of a local cavity, and in the vicinity of the cavity to produce a stress field, resulting in the induced shear stresses to open the front of the cracks so that the cracks propagate at the interface [62], which reduces the strength of the ice adhesion, icing can be easily slipped off. Table 3 summarised the study of Interfacial microzonation modulus difference surface prepared by different design methods.

4.1 Elastomeric coatings

The stress required for ice to move on the surface ranges from 0.2 to 10 kPa, and the normal or tangential critical separation force required to separate an adherent rigid mass (e.g., ice) from an elastomeric coating can be derived from the fracture mechanics as the following law: $F_c \propto \sqrt{W_{ad}E/t}$, with F_c being the critical separation force, Wad being the interfacial adhesion energy, E and t being the modulus of elasticity of the elastomeric layer and the thickness respectively [26]. This suggests that lowering the elastic modulus of the coating can induce stress localization at the ice-material elastic interface, resulting in an interfacial weakening behavior to achieve a crack-induced de-icing strategy that effectively reduces the strength of ice accumulation adhesion. The elastomer

Table 3 Interfacial microzonation modulus difference surface prepared by different design methods

Design method	Material	Adhesion strength	Literature
Elastomeric coatings	gel particles with lower modulus of elasticity composed of PDMS/gel particles two-phase materials	< 10 kPa	[62]
	polyurethane (PU) embedded with various soluble oily polymers	< 10 kPa	[63]
	dispersing candle ash particles into a silicone rubber matrix	18 kPa	[64]
	a sponge-structured low modulus of elasticity (< 1 MPa) PDMS	0.9 kPa	[65]
	rigid nanocomposites with the elastic modulus of GPa scales (SiO2NPs, 68.9 GPa) into the surface layer of elastomers (PDMS, 2.7 MPa)	10.5 kPa	[66]
	porous PDMS sponges sandwiched between a protective, dense PDMS layer and a textured metal microstructure	< 5.3 kPa	[67]
	multiscale interpenetrating reinforcing method	< 20 kPa	[68]
Low interfacial toughness coatings	a new surface called magnetic slippery surface in two forms of Newtonian fluid (MAGSS) and gel structure (Gel-MAGSS)	2 kPa	[69]

soft coating is a stress-localized viscoelastic material, which forms cracks at the ice-material interface when shearing the ice, generating a localized stress field so that the shear stresses continue to advance the cracks at the interface, ultimately separating the ice from the material.

Reducing the shear modulus of various elastomers can be achieved by lowering the crosslink density of the structure, Golovin [63] first used polyurethane (PU) embedded with various soluble oily polymers to prepare soft anti-icing coatings with a low crosslink density, low elastic modulus and high slip with an ice build-up adhesion strength of less than 10 kPa. Using low elastic modulus coatings further modified to produce localized stressing, Irajizad [62] prepared gel particles with lower modulus of elasticity composed of PDMS/gel particles two-phase materials by using PDMS as the substrate, and the adhesion strength of the coated cumulus ice was less than 10 kPa in all cases, and it was found that debonding (Fig. 10a), always occurs around the gel particles first, and then cracks rapidly extend to the entire interface. Jamil [64] prepared a low elastic modulus superhydrophobic coating by dispersing candle ash particles into a silicone rubber matrix, which simultaneously utilized low elastic modulus, superhydrophobicity and Irajizad-like effects of localized stresses with an ice accumulation adhesion strength of only about 18 kPa. He [65] prepared a sponge-structured low modulus of elasticity (< 1Mpa) PDMS coating by the template method. This structure is full of internal cavities but has a flat surface, and when external forces are applied to the ice, the deformation of the internal cavities causes debonding at the interface between the ice and the coating, which greatly reduces

the apparent ice adhesion strength compared to the solid homogeneous PDMS coatings, which have a minimum ice adhesion strength of only 0.9 kPa.

In addition to the local stressing of the elastomeric material, which plays an important role in the de-icing process, the "springboard effect" formed by the bouncing mechanism also effectively inhibits the pre-icing behavior. The upward force of the elastic substrate completely separates the droplets by converting the surface energy into kinetic energy. Weissensee [71] explains the springboard effect and shows that the contact time of a water droplet impacting an elastic superhydrophobic surface is reduced by a factor of 2 compared to an equivalent rigid surface. Harmonic motion is also observed on the elastic/flexible substrate as it oscillates at normal frequencies after droplet impact and can cause droplets in a pancake bounce to dislodge prematurely from the surface. Vasileiou [70] pioneered the method of bouncing of ice crystals after icing of elastomeric coatings by constructing micro-nano structures on a certain flexibility of low-density polyethylene film. The surface of flexible substrate composite with micro-nano structures was obtained. Due to the effective absorption and rectification of droplet kinetic energy by the flexible substrate, the supercooled droplets can bounce off the flexible substrate even after icing (Fig. 10b). Compared with other superhydrophobic coatings, elastomeric superhydrophobic surfaces are characterized by short contact times, less disruptive weaving structures and minimal droplet spreading without rupture.

The application of low elastic modulus coatings in harsh environments is limited by the degradation of
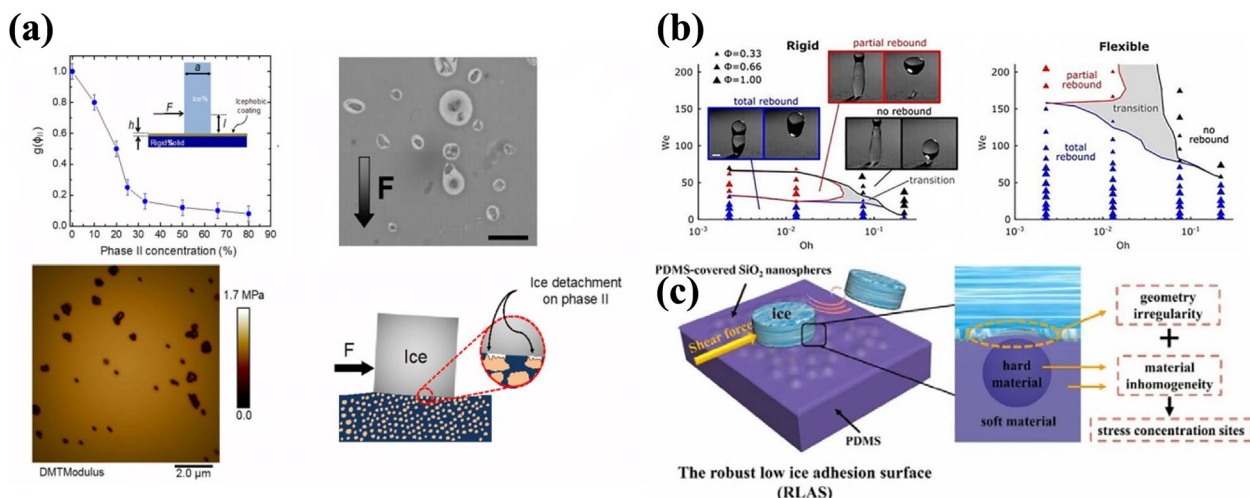

Fig. 10 **a** Ice cover easily detaches from the second phase due to interfacial cracks created by the second phase under micro external forces [62]; **b** Rapid rebound of droplets on all elastic substrate contacts, slow or no rebound on other substrate parts [70]; **c** Rigid Nanocomposites Generate Stress Concentration Sites [66]

mechanical robustness, where stress concentration due to surface hardening of elastomers contributes to cracking of the elastomeric surface layer due to material inhomogeneities and geometrical irregularities. For coatings with fracture-weakening interfacial effects, the synergistic maintenance of ultra-low ice adhesion and mechanical robustness contributes to the practical application of elastomeric coatings. Jiang [66] revealed the effect of the location of stress concentration due to material inhomogeneity (stiffness mismatch) and geometrical irregularities on the reduction of ice adhesion strength. Rigid nanocomposites with GPa-scale modulus of elasticity were added to the surface layer of elastomers to introduce stress concentration sites and obtain a robust low ice adhesion surface (RLAS). The nanocomposite surface layer is rich in potential crack budding sites and hard NPs (Fig. 10c), which significantly reduces the adhesion strength while providing more than two times higher mechanical stiffness than that of pure elastomers. Chen [67] showed the presence of a protective porous PDMS sponge interlayer between the dense PDMS layer and the textured metal microstructure. The combination of high stiffness anchored by the structured metal surface and low stiffness of the PDMS coating imparts excellent icephobicity to the sandwich-like structure, and the porosity and modulus of elasticity result in a significant increase in surface durability over a single PDMS coating. Wang [68] taking inspiration from subcutaneous tissues, proposed a multi-scale interpenetrating reinforcement method to interlock and strengthen the ultra-smooth hydrophobic interface, introducing epoxy resin molecular chains into the PDMS gel to form a high-strength molecular network with adjustable elastic modulus, and doping solid lubricant, so that the surface can more firmly hold the liquid lubricant and form a solid-liquid dual lubrication effect, which combines the super-slip interface with the crack-inducing interface to minimise the elastic deformation and fracture initiation stress threshold during ice peeling.

4.2 Low interfacial toughness coatings

Golovin [72] proved that when the icing area reaches a certain level, the external force required for de-icing is independent of the area, and is related to the interfacial toughness of the material and the bonding strength between the substrate and the ice, which can be adjusted by adjusting the bonding strength. bond strength, and that the interfacial toughness can be altered by modulating the shear modulus and thickness of the material to achieve large-area de-icing (Fig. 11a). Developed for the first time a low interfacial toughness (LIT) anti-icing coating that can be used to de-ice large areas (Fig. 11b). Low interfacial toughness (<1 J/m^2) PDMS was coated onto an aluminum alloy plate of about 1 m$\times$1 m. After forming 10 mm of ice at -7 °C and placing the plate at an inclination of 98°, the ice came off by its own gravity in the absence of any other external force (Fig. 11c). Irajizad [69] introduced the concept of magnetic slippery surfaces, which utilise magnetic forces to induce liquid-liquid inhomogeneous interfaces. These surfaces exhibited extreme ice repellency with an ice adhesion strength of 2 kPa. however, the liquid volatile nature of these
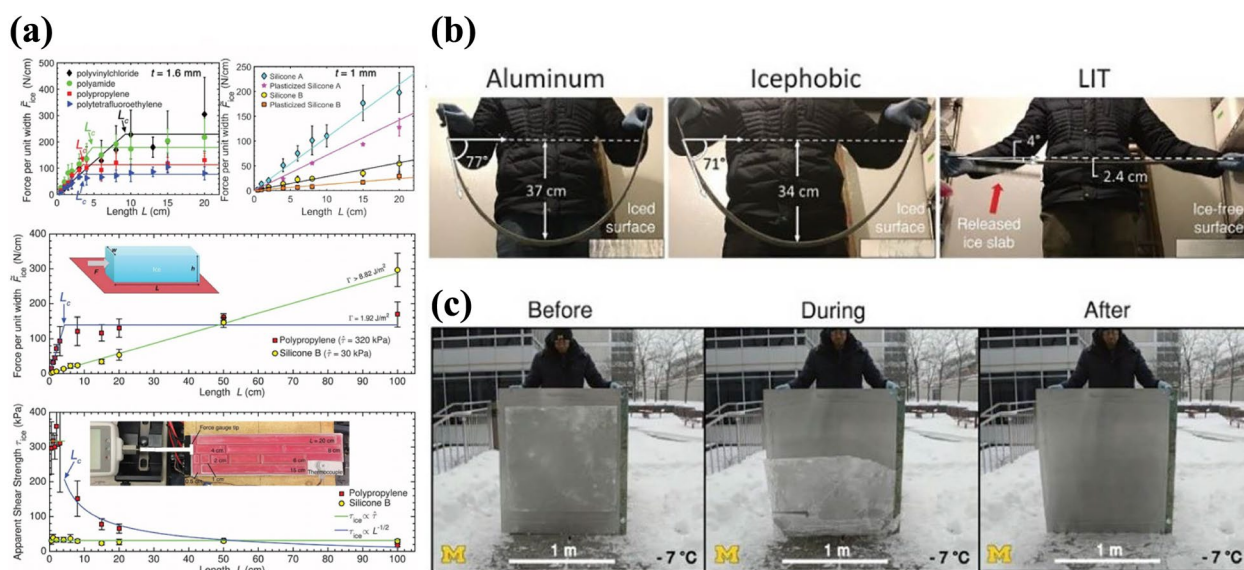

Fig. 11 **a** Strength- versus toughness-controlled fracture [72]; **b** LIT materials are only 1/15th as tough as aluminum; **c** Large-scale testing of LIT materials [69]

surfaces limited their mechanical durability for long-term applications.

Elastomeric coatings and low-toughness coatings based on differential microregion modulus can create stress localisation at the interface, promoting the generation of microcracks and ductile propagation, and reducing the ice adhesion strength to as low as 2 kPa. Meanwhile, in order to enhance the mechanical properties, the above studies have increased the mechanical strength by more than two times through rigid nanoparticle composites, sponge intercalation, network interpenetration reinforcement, and functional composites. The study shows that when the accumulated ice reaches a certain size, the de-icing has nothing to do with the size of the external force, but only depends on the interfacial toughness, which makes the micro-area modulus-controlled coatings have the prospect of large-scale de-icing applications. However, at present, the R&D and preparation process of this type of coating technology is relatively complex, and the cost of PDMS materials is relatively high, and the mechanical strength and durability need to further satisfy the long-lasting requirements in complex service environments. These coatings are mostly utilised as surface anti-icing methods for big structural components, such as aircraft, ships, offshore wind power, towers, and other equipment, because of their low hardness qualities.

5 Multi-factor synergistic coupling design

Due to the limitations of material properties and preparation processes, passive anti-icing surfaces have problems such as single function, insufficient long-term stability, and poor anti-icing/de-icing effects under extreme temperature and humidity conditions. In recent years, researchers have demonstrated that the combination of passive de-icing and active de-icing multiple composite anti-icing can improve the stability and practicality of the material.

5.1 Photothermal composites

Photothermal composite materials are based on conventional superhydrophobic or lubricated surface to add photothermal materials for modification, which photothermal materials require a high solar absorption rate, and does not affect the original characteristics of the coating, according to the material can be divided into carbon fibers, carbon nanotubes and other carbon-based photothermal conversion materials, metal NPs such as Fe_3O_4, TiN and other semiconductor materials. Current research is no longer limited to the coupling of two characteristics, multi-factor synergistic coupling design methods and processes are gradually diversified and efficient. Liu [73] used silicone oil (SO) as a lubricating matrix filled with porous silica aerogel (SiO_2 aerogel), carbon nanotubes and silicone rubber mixed with beeswax to obtain the composite of the micro-nano structured, self-lubricating and combined photo-thermal anti-icing coating, WCA = 162°, WSA = 4.8°, icing delay time as high as 596 s, only one solar irradiation surface temperature rises rapidly to 85° C, ice crystals can be melted in 150 s. In addition, the beeswax phase change material endows the coating with efficient self-healing properties. Ultra-black coatings with more than 99% absorbance are widely used in the aerospace, optical instrument and solar energy industries. However, the high-temperature preparation conditions of ultra-black coatings limit their application prospects. Lin [74] used laser etching to achieve a new method of preparing carbon nanotube-filled resin-based composite ultra-black coatings based on carbon nanotubes at room temperature. After laser etching removes the pure resin film from the surface of the coatings, the light-contact interface is changed from air/resin to air/
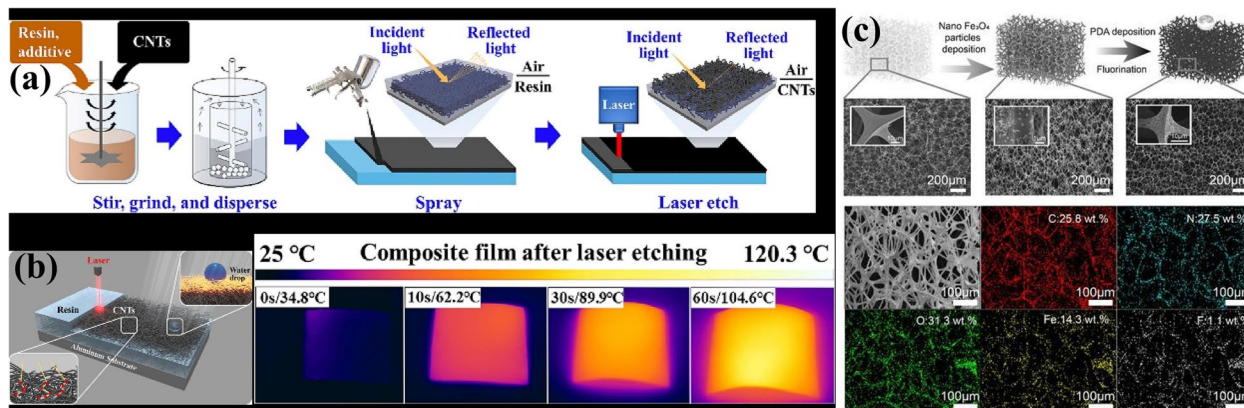

Fig. 12 a IR thermal images of the pure resin film, the composite film before etching [74]; **b** The composite film after laser etching under xenon lamp irradiation [74]; **c** The structure and components of PSP-SPONGE obtained by depositing Fe_3O_4 NPs and polydopamine

CNTs (Fig. 12a), and the coating's highest average light absorbance is 99.49%. At the same time, the surface of the coating was transformed from smooth to porous microstructure, which significantly increased the photothermal conversion and improved the surface roughness and hydrophobicity (Fig. 12b). Yu [75] has developed a photothermal superhydrophobic polyurethane sponge (PSP-Sponge) (Fig. 12c), which is fluorided by depositing Fe_3O_4 NPs and polydopamine for rapid anti-icing and de-icing under weak sunlight. Utilizing the insulating properties of the porous PSP-SPONGE, water droplets on the surface of the PSP- Sponge will never freeze under weak 0.3 kW/m^2 ("0.3 suns") sunlight in humid environments at -30 °C, while under "1 sun" exposure the ice will completely melt in 18 min. In addition, PSP- Sponge has excellent self-cleaning and self-repairing properties to cope with complex and changing natural environments, ensuring long-lasting anti-icing and de-icing performance. In a humid outdoor environment at -30 °C, snow on the surface of PSP- Sponge can melt in "0.5 suns" of sunlight.

Photothermal materials often have weakened heat production capacity due to particle loss during service, and suitable materials can be chosen to enhance or replace the function of photothermal particles. Lee [76] added carbonyl iron particles to PDMS, obtained magnetically responsive cilia matrix with the help of neodymium magnets, and coated MWCNTS NPs on the top layer to prepare multifunctional anti-icing coatings with magnetically responsive photothermal composite cilia arrays (MRPAs). The MRPA undergoes immediate reversible structure-driven motion under an external magnetic field, and this cilia state transition mechanism can actively remove liquid droplets while ensuring superhydrophobic stability. 97.8% or more spectral absorption provides efficient photo-thermal conversion, and the icing time is 105 s in the absence of light, and no significant icing behavior is observed under light conditions. Liu [77] formed brominated carbon nanotubes on the surface of PDMS film and grafted PFMA brushes by SI-CuCRP method to form PFMA/CNTs composite PDMS superhydrophobic films with organic-inorganic composite enhancement structure. After 120 sandpaper rubbings, the composite PDMS film with a contact angle of 170° still has good superhydrophobicity and can continue to dehydrate. It also has good abrasion resistance and self-healing ability, and the delayed icing time and ice adhesion strength are 872 s and 61.9 kPa, respectively, which show efficient anti-icing performance. In addition, due to the photothermal conversion ability of carbon nanotubes, the PFMA/CNTs composite PDMS superhydrophobic films showed excellent deicing effect under near-infrared irradiation. Guo [78] used
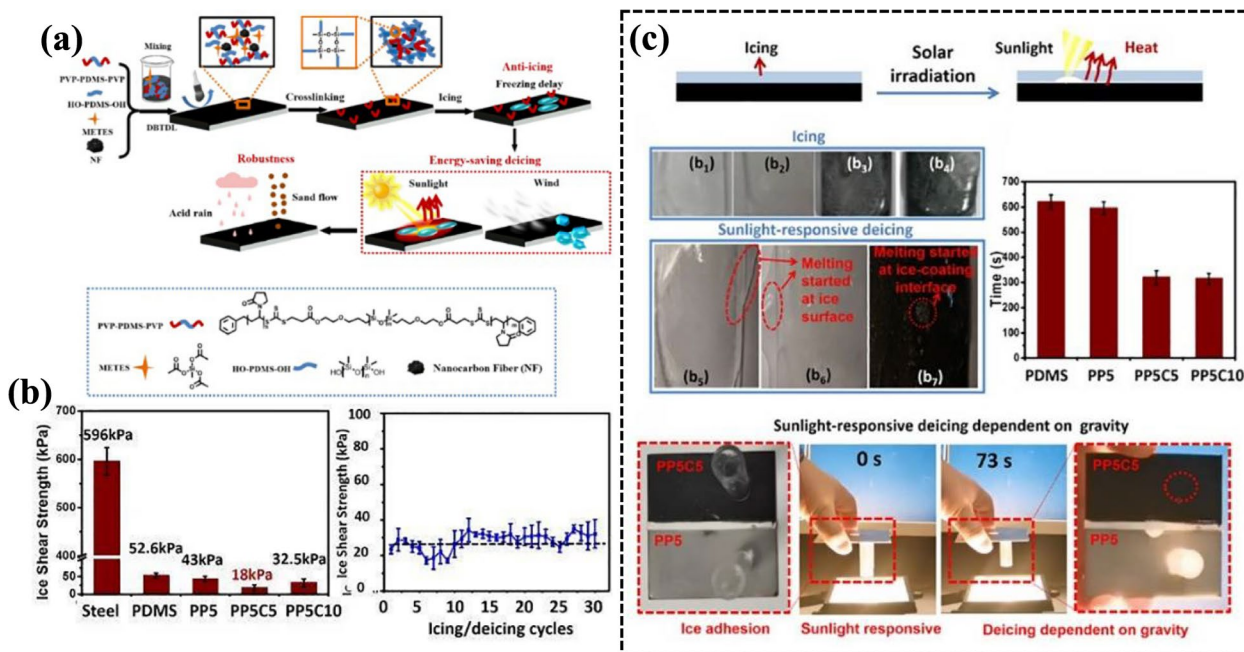

Fig. 13 **a** Hydrolysis catalyzed by the cross-linker METES at 70 °C DBTDL produces a condensation reaction of HO-PDMS-OH and Si-OH groups to form the designed co-polymerized network; **b** Ice adhesion strength is only 18kPa, and the surface temperature of the coating can reach 46℃ under sunlight irradiation; **c** The photothermal effect of the overlying ice melts within 300 s and slides off by gravity [78]

a combination of photothermal carbon nano-fibers, PDMS, and hydrophilic polyvinylpyrrolidone (PVP) to obtain PP5C5 coatings (Fig. 13a), which formed a reduced internal Hydrophilic PVP chain segments with lowered freezing point effectively prevented the formation of ice nuclei, and the carbon fibers absorbed sunlight to generate heat for de-icing (up to 10 °C/min), while further reducing the ice adhesion strength on the surface of the PDMS-based coating to 18 kPa (Fig. 13b), and the accumulated ice was removed under sunlight, relying on natural conditions such as wind and gravity only. In addition, the new coating has good stability, and after 30 cycles of anti-icing tests, there is no significant change in the ice adhesion strength. the ice layer on PDMS and PP5 surfaces started to melt on layer surfaces, while melt at the location contact with the PP5C5 and PP5C10 coating with a much faster melting speed than PDMS and PP5. Moreover, the sunlight-responsive deicing process of PP5C5 coating was depended on ice gravity and spent only 73 s (Fig. 13c).

5.2 Electro-thermal composite materials

Photo-thermal composite materials require continuous sunlight or infrared light to achieve a stable photo-thermal conversion effect, the light requirements of the service environment make its application range is limited. Electrothermal composites can be independent of the service environment, and faster heating and de-icing. Sullivan [79] developed a composite electrothermal anti-icing coating consisting of a thin-film electric heater and a superhydrophobic top coating. The coating was applied to a stainless-steel substrate by a simple multilayer spray process. The heating film consisted of a layer of copper-based epoxy resin insulated between layers of PDMS elastomer. Excellent thermal stability was demonstrated at temperatures up to 100 °C. The SiO_2-PDMS superhydrophobic top coating had a WSA of 164°, a hysteresis angle of 3° and an 83% reduction in ice adhesion strength compared to the substrate. The minimum surface power density of 0.34 W/cm^2 at -20 °C room temperature induced water droplets to roll off the 45° inclined superhydrophobic surface, achieving complete ice protection. However, the interfacial thermal
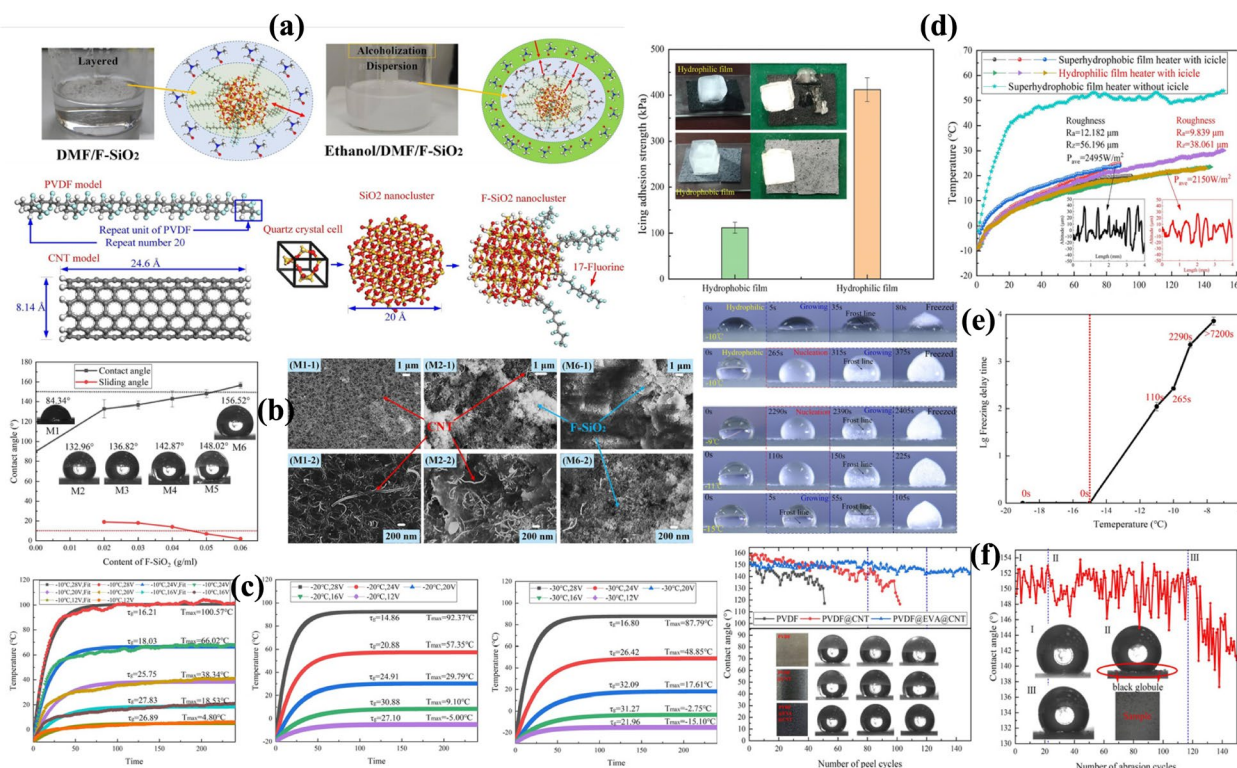

Fig. 14 **a** The dispersion behavior and modeling process of PVDF, CNT, SiO_2 nanocluster and F-SiO_2 nanocluster; **b** The static contact angles and surface topography of the superhydrophobic film heater with different concentrations of spraying solution; **c** The fitting electrothermal performance curves of the heating stage at the environment temperature of -10 °C, -20 °C, and -30 °C; **d** The heating and de-icing effect of both films under loading power when the environmental temperature is -10 °C; **e** The freezing process delay time of droplet on the superhydrophobic surface with different temperatures; **f** The tape stripping and the wear resistance test of superhydrophobic film, including PVDF film, PVDF@CNT film, and PVDF@EVA@CNT film [80]

resistance between the electrothermal and superhydrophobic zones during the preparation of electrothermal superhydrophobic composite coatings can affect the heat transfer efficiency. Wang [80] prepared a novel integrated superhydrophobic membrane heating coating by combining solution casting and wet film spraying. The PVDF model contains 20 repeat units and the length of CNT model is 24.6 Å. Based on quartz crystal cell, the SiO_2 nanocluster and $F-SiO_2$ nanocluster were constructed applying the nanocluster modeling tool (Fig. 14a). The CNT is uniformly distributed to form a dense conductive network on the untreated film surface, realizing an excellent electrothermal function (Fig. 14b). The superhydrophobic membrane heating coating has the same heating effect as hydrophilic membranes at room temperature of -30 °C at a load power of 3018 W/m^2, the peak temperature can reach about 87.79 °C (Fig. 14c). The superhydrophobic film heater with an ice adhesion strength of 112 kPa has a 72.8% reduction over the hydrophilic film heater (Fig. 14d). Compared with the conventional electric heating coating, the integrated superhydrophobic film heater can save up to 27.37% of energy consumption for de-icing at -10 °C. The anti-icing function of superhydrophobic film heater is effective when the film temperature is above −13 °C. However, the coupled electrothermal function can control film temperature and greatly lengthen the freezing time (Fig. 14e). In addition, the superhydrophobic durability was enhanced by the interpenetrating behavior between PVDF, EVA, CNT and $F-SiO_2$ (Fig. 14f).

Conventional electric heating coatings suffer from high energy consumption and low thermal efficiency, and graphene's ultra-high electrical conductivity also offers the possibility of energy saving and efficiency enhancement for electrically heated coatings. Zeng [81] built a coupled system combining superhydrophobic coatings with graphene electric heaters, and this coupled system saves 60% of the energy compared to conventional wire heating, and the energy consumption for anti-icing saves 60% of the energy compared to graphene alone. heating, the anti-icing energy consumption was saved by 21% and the de-icing efficiency was improved by 250% compared to graphene heating alone. In addition, the "honeycomb" and "island" structures give the coatings better anti-icing effect and mechanical stability. Chen [82] verified the semi-interpenetrating structure of conductive graphene ("HCG") siloxane hydrophobicity in the Finnish Arctic Circle. HCG) siloxane hydrophobic coating in the Finnish Arctic Circle, and the developed coating has excellent anti-icing performance at a power of about 310 W/m^2. In addition, the coating exhibited satisfactory de-icing performance at a power of about 570 W/m^2 and successfully removed the accumulated ice in about 10 min.

Zhao [83] proposed a multifactorial coupled anti-icing/de-icing coating with superhydrophobic passive anti-icing and electro-thermal/photo-thermal active de-icing performance. The multifunctional anti-icing/de-icing coating was prepared using fluorinated epoxy resin and carbon/PTFE particles, and the synergistic ice-removal mechanism was verified by characterising the different freezing states of water droplets on the surface: repelling water droplets before freezing occurs, delaying icing during freezing, and significantly reducing ice adhesion after freezing by the microscale water film generated by heating.

5.3 Phase change composites

The thermoregulatory ability of phase change materials to absorb and release large amounts of latent heat can delay ice crystal nucleation and accelerate the process of ice melt shedding. Heat storage and release is driven by the temperature difference, the coating can be defined as having a "temperature switch" effect. Phase change anti-icing coatings have been studied relatively extensively, and their performance has been verified and applied numerous times. Combining phase change materials with other passive anti-icing strategies (e.g. self-lubricating coatings) can improve the anti-icing performance. However, the energy storage efficiency of phase change materials can be severely compromised after many alternating cycles of use due to leakage, failure, etc., which puts higher requirements on the modification and encapsulation of phase change materials. Yuan [84] n-tetradecane and nucleating agents to obtain the desired phase change temperature to apply it to Permanent Room Temperature Vulcanised (PRTV) silicone rubber, prepared phase change microcapsules (MPCM/PRTV) coatings (Fig. 15a). The spectrum of MPCMs contained all the characteristic absorption peaks of n-tetradecane and MUF resin, manifesting that n-tetradecane has been microencapsulated into MUF resin shell successfully with no reaction between the core and wall materials (Fig. 15b). N-tetradecane as the core material and C36 as the nucleating agent, the prepared microcapsules have suitable phase transition temperature and higher latent heat (Fig. 15c). The release of latent heat from the MPCM in the coating and surface roughening synergistically extend the freezing time of water droplets from 1381 to 3432 s. In addition, the MPCM in the coating can repeatedly absorb and release energy and maintain its integrity without cracking during icing/thawing cycles, and the anti-icing/de-icing properties of the MPCM/PRTV coatings showed durability (Fig. 15d). Shamshir [85] prepared ice-phobic by impregnating an elastomeric matrix containing PEG-PDMS copolymers with PCM microcapsules. The content of PCM microcapsules also directly
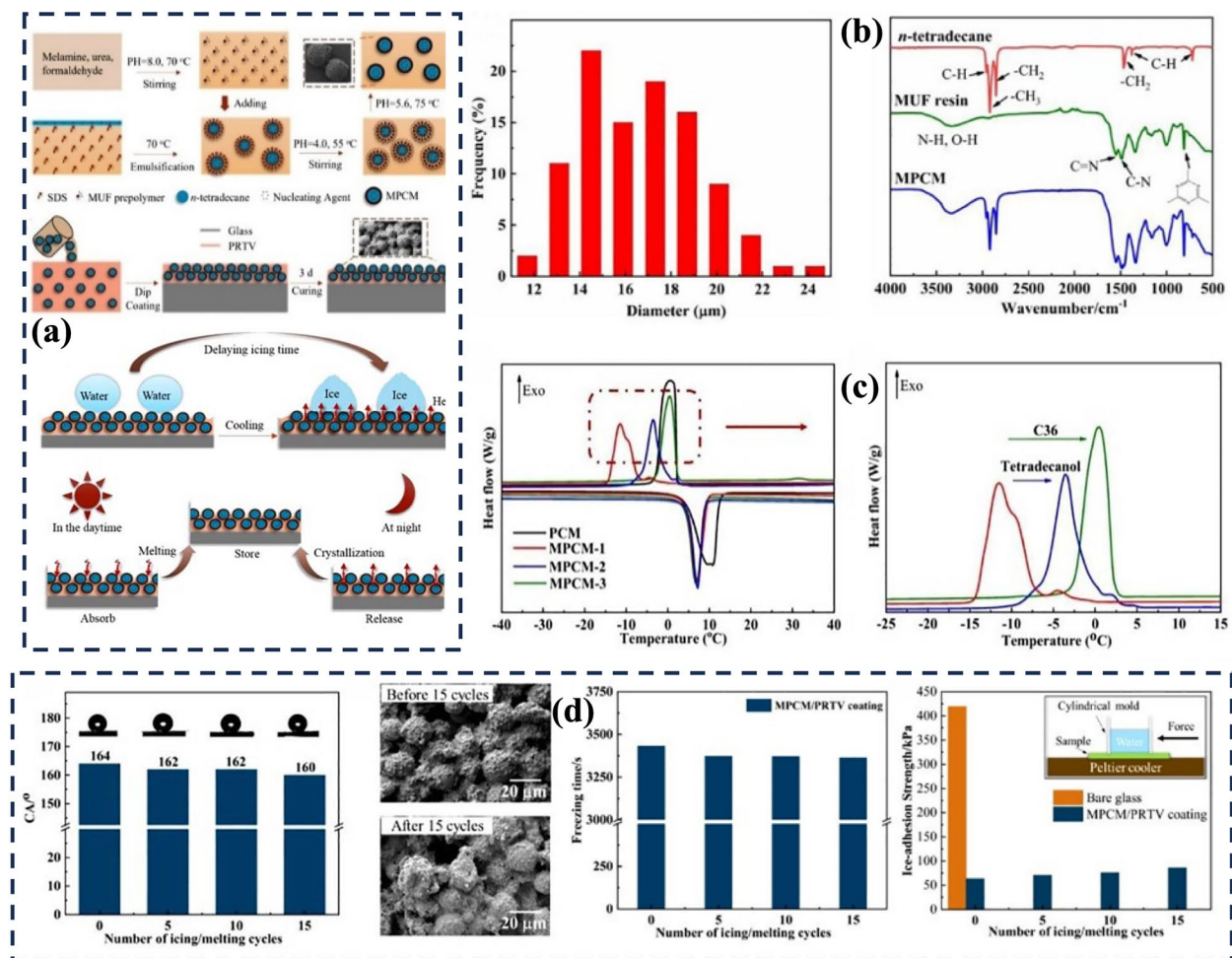
Fig. 15 a Schematic fabrication of MPCMs via in-situ polymerization and MPCM/PRTV coating by dip coating methods; **b** Size distribution of MPCMs and FTIR spectra of n-tetradecane, MUF resin and MPCMs; **c** DSC heating and freezing curves of n-tetradecane and MPCMs with and without nucleating agents; **d** Variation in CA, micrographs, freezing time of water droplet, ice-adhesion strength of MPCM/ PRTV coating before and after 15 de-icing cycles [84]

affects the self-lubricating properties and latent heat release properties of the matrix containing PEG-PDMS copolymer, and the high content contributes to a further reduction in ice adhesion.

6 Conclusions and outlook

At present, the main R&D direction of anti-icing coatings is still based on the previous biomimetic materials, such as the earliest superhydrophobic surface developed by the lotus leaf-like effect, and the preliminary discovery of biomimetic antifreeze proteins. The evolution of biological functions in nature always provides researchers with a constant source of inspiration, and more biomimetic coatings will become a reality with the continuous development of new materials and new processes. In this article, the design mechanisms of anti-icing coatings are classified into superhydrophobicity, sacrificial physicochemical material release, microregion modulus differentiation, and multifactorial coupling from the perspective of icing process and anti-icing mechanism, focusing on the summary and analysis of the latest advances in the design and preparation of coatings of each mechanism, and discussing the performance advantages and shortcomings of surfaces of the corresponding mechanisms.

Compared with active de-icing, the passive anti-icing method of constructing anti-icing and ice-phobic surfaces can form a systematic de-icing effect in the whole process before, during, and after icing. Superhydrophobic surface coatings form a low contact angle and a small contact area at the interface through low surface energetics and superhydrophobicity, and micro-nano structured superhydrophobic surfaces are at the expense of the thickness of the samples, and the

Zhao *et al. Surface Science and Technology*   (2024) 2:2

Page 22 of 24

application of the process of the superhydrophobic roughness structure, especially nanostructures, is prone to mechanical damage. Mechanical damage, sacrificial physical and chemical effects of surface loss also affect the service time limit, self-repair, self-supplementation, self-healing and other regenerative functions greatly enhance the coating to the market hope. The static supercooled water on the surface in Cassie-Baxter state is very easy to roll off, effectively inhibiting the solid-liquid interface icing behavior. However, droplets are always present in high humidity environments, and dynamic supercooled water is often used in practical applications. When in contact with superhydrophobic surfaces, it is very easy to change to the Wenzel adhesion state, where the micro-nano structures lead to the anchoring effect of droplet icing instead. Therefore, the promotion of Cassie-Baxter steady state is a prerequisite for the large-scale application of anti-icing coatings.

The application prospect of anti-icing coatings is extremely broad, and there is an urgent need in the fields of infrastructure construction and transport. However, the differences in working conditions, substrates, and functions make the coating service complex, variable, and demanding, which puts forward higher requirements for the functional composability of the coating. Therefore, there is a need for more in-depth investigation of the mechanism of supercooled water nucleation, growth, phase transition, adhesion and other processes, to discover the relationship between the surface components of the coating, the structure, the mechanical properties of the micro-zone exists between the law, which will help to target the establishment of a multi-factor synergistic coupling mechanism.

At present, although there are quite a number of types of anti-icing coatings in the laboratory was developed and prepared, but there is no more mature products with large-scale landing applicability, which is due to the preparation process is relatively cumbersome, the application of the site coating process requirements, such as bionic antifreeze proteins, such as the cost of production and maintenance of the material is still relatively high, and gradually optimize the preparation process and control of raw material costs can be reduced to the limits of the production and application of the results to help marketable application of the results.

Credit authorship contribution statement
We would like to declare on behalf of my co-authors that the work described was original research that has not been published previously and is not under consideration for publication elsewhere, in whole or in part.

Author contributions
Zhongxian Zhao: Completed the writing of the main body of the paper and revised the responses to the review comments. Xiaofeng Li: Mainly proofreading the content structure of the thesis and the presentation of specialised knowledge points. Wenge Li: Mainly to proofread the paper's anti-icing mechanism and design classification. Minghui Liu: Professional guidance mainly on thesis on anti-icing coatings and materials for environmental pollution. Zhaowei Hu: Guidance on the formatting of the writing in the thesis primarily. Tao Jiang: A large amount of literature related to the study of anti-icing coatings has been collected and collated. Haoran Wang: Mainly assisted in the collection and collation of literature related to the study of anti-icing coatings. Yuantao Zhao: As a corresponding author, he/she mainly provides guidance on the overall framework structure of the paper and is responsible for reviewing and proofreading submissions and responses.

Declarations

Competing interests
The authors declare that they have no known competing financial interests or personal relationships with other people or organizations that could have appeared to influence the work reported in this article.

Author details
[1]College of Ocean Science and Engineering, Shanghai Maritime University, Shanghai 201306, China. [2]Engineering Training Centre, Shanghai Maritime University, Shanghai 201306, China. [3]School of Merchant Marine College, Shanghai Maritime University, 1550 Haigang Avenue, Pudong New Area, Shanghai 201306, China. [4]Shanghai Songjiang Landscaping & City Appearance Administrative Bureau, Shanghai 201699, China.

References
1. Zhu DY, Zhang FK, Pei RN et al (2016) Study on critical ice shape determination method and its effect on aerodynamic characteristics. Acta Aerodyn Sin 34(06):714–720. https://doi.org/10.7638/kqdlxxb-2015.0217
2. Xiao Z (2021) Research on anti-icing characteristics of wear-resistant superhydrophobic coating and its mechanism. Doctoral dissertation. Southeast University. https://doi.org/10.27014/d.cnki.gdnau.2021.003765
3. Emery AF, Siegel BL (1990) Experimental measurements of the effects of frost formation on heat exchanger performance. 139:1–7. https://api.semanticscholar.org/CorpusID:136364745
4. Lu JY, Wang JJ (2014) Research progress of anti-icing coatings. Coat Prot 35(08):37–41. https://doi.org/10.3969/j.issn.1672-2418.2014.08.016
5. Zhao YJ, Yan ZX, Su JM et al (2021) Advances in bionic anti-icing surfaces. Surf Technol 50(10):29–39. https://doi.org/10.16490/j.cnki.issn.1001-3660.2021.10.003
6. Khadak A, Subeshan B, Asmatulu R (2021) Studies on de-icing and anti-icing of carbon fiber-reinforced com-posits for aircraft surfaces using commercial multifunc-tional permanent superhydrophobic coatings. J Mater Sci 56(4):3078–3094. https://doi.org/10.1007/s10853-020-05459-9
7. Lian Z, Xu J, Wang Z et al (2020) Biomimetic superlyophobic metallic surfaces: focusing on their fabrication and applications. J Bionic Eng 17(1):1–33. https://doi.org/10.1007/s42235-020-0002-y
8. Deng CH, Jin RS, Qi DM et al (2023) Preparation of anti-icing/deicing functional composite materials and its research progress. Acta Mater Compos Sin [09-17]:1–14. https://doi.org/10.13801/j.cnki.fhclxb.20230302.001

Zhao et al. Surface Science and Technology   (2024) 2:2

Page 23 of 24

9. Xu S, Zhou Z, Feng L et al (2021) Durability of pavement materials with exposure to various anti-icing strategies. Processes 9(2):291. https://doi.org/10.3390/pr9020291

10. Wu DH, Liu WJ, Wu B et al (2022) Progress of anti-icing materials in extreme low temperature environment. Surf Technol 51(06):1–13. https://doi.org/10.16490/j.cnki.issn.1001-3660.2022.06.001

11. Cui MM, Huang H, Wu HX et al (2023) Achieving superhydrophobicity of Zr-based metallic glass surface with anti-corrosion and anti-icing properties by nanosecond laser ablation and subsequent heat treatment. Surf Coat Technol 475:130159. https://doi.org/10.1016/j.surfcoat.2023.130159

12. Shi P, Chen H, Gong HQ et al (2008) Preparation of superhydrophobic surfaces. J Funct Polym 21(2):230–236. https://doi.org/10.3969/j.issn.1007-1865.2014.20.046

13. Thi QH, Man P, Liu H et al (2023) Ultrahigh lubricity between two-dimensional ice and two-dimensional atomic layers. Nano Lett 23(4):1379–1385. https://doi.org/10.1021/acs.nanolett.2c04573

14. Lee HJ (2012) Design and development of anti-icing textile surfaces. J Mater Sci 47(13):5114–5120. https://doi.org/10.1007/s10853-012-6386-2

15. Cao YZ, Lu YM, Liu N et al (2022) Multi-applicable, durable superhydrophobic anti-icing coating through template-method and chemical vapor deposition. Surf Interfaces 32:102100. https://doi.org/10.1016/j.surfin.2022.102100

16. Wu YL, Shu X, Yang Y et al (2023) Fabrication of robust and room-temperature curable superhydrophobic composite coatings with breathable and anti-icing performance. Chem Eng J 463:142444. https://doi.org/10.1016/j.cej.2023.142444

17. Zhu GY, Su J, Yin CX et al (2023) Constructing a robust ZIF-7 based superhydrophobic coating with the excellent performance in self-cleaning, anti-icing, anti-biofouling and anti-corrosion. Appl Surf Sci 622:156907. https://doi.org/10.1016/j.apsusc.2023.156907

18. Fu K, Lu C, Liu YB et al (2021) Mechanically robust, self-healing superhydrophobic anti-icing coatings based on a novel fluorinated polyurethane synthesized by a two-step thiol click reaction. Chem Eng J 404:127110. https://doi.org/10.1016/j.cej.2020.127110

19. Zhu TX, Cheng Y, Huang JY et al (2020) A transparent superhydrophobic coating with mechanochemical robustness for anti-icing, photocatalysis and self-cleaning. Chem Eng J 399:125746. https://doi.org/10.1016/j.cej.2020.125746

20. Hong SQ, Wang RT, Huang XB et al (2019) Facile one-step fabrication of PHC/PDMS anti-icing coatings with mechanical properties and good durability. Prog Org Coat 135:263–269. https://doi.org/10.1016/j.porgcoat.2019.06.016

21. Li J, Jiao WC, Jin HZ et al (2023) Robust polyurea icephobic coatings with static large-scale de-icing and dynamic anti-icing performance. Chem Eng J 147339. https://doi.org/10.1016/j.cej.2023.147339

22. Huang XC, Sun M, Shi X et al (2023) Chemical vapor deposition of transparent superhydrophobic anti-Icing coatings with tailored polymer nanoarray architecture. Chem Eng J 454(1):139981. https://doi.org/10.1016/j.cej.2022.139981

23. Zheng ZH, Liao CC, Xia YR et al (2021) Facile fabrication of robust, biomimetic and superhydrophobic polymer/graphene-based coatings with self-cleaning, oil-water separation, anti-icing and corrosion resistance properties. Colloids Surf A Physicochem Eng Asp 627:127164. https://doi.org/10.1016/j.colsurfa.2021.127164

24. Shen YZ, Jin MM, Wu XH et al (2019) Understanding the frosting and defrosting mechanism on the superhydrophobic surfaces with hierarchical structures for enhancing anti-hosting performance. Appl Therm Eng 156:111–118. https://doi.org/10.1016/j.applthermaleng.2019.04.052

25. Pan R, Zhang HJ, Zhong ML (2021) Triple-scale superhydrophobic surface with excellent anti icing and icephobic performance via ultrafast laser hybrid fabrication. ACS Appl Mater Interfaces 13(1):1743–1753. https://doi.org/10.1021/acsami.0c16259

26. Ma C, Chen L, Wang L et al (2022) Condensation droplet sieve. Nat Commun 13:5381. https://doi.org/10.1038/s41467-022-32873-1

27. Zhang HL, Guo ZG (2023) Recent advances in self-healing superhydrophobic coatings. Nano Today 51:101933. https://doi.org/10.1016/j.nantod.2023.101933

28. Nishino T, Meguro M, Nakamae K et al (1999) The lowest surface free energy based on CF_3 alignment. Langmuir 15(13):4321–4323. https://doi.org/10.1021/la981727s

29. Xie Q (2021) Research on anti-icing performance and mechanism of action of organosilicon/epoxy resin coating. Doctoral dissertation. Harbin Engineering University. https://doi.org/10.27060/d.cnki.ghbcu.2021.000080

30. Simpson JT, Hunter SR, Aytug T (2015) Superhydrophobic materials and coatings: a review. Reports on progress in physics. Phys Soc (Great Britain) 78(8):086501. https://doi.org/10.1088/0034-4885/78/8/086501

31. Si YF, Guo ZG (2015) Superhydrophobic nanocoatings: from materials to fabrications and to applications. Nanoscale 7(14):5922–5946 (https://api.semanticscholar.org/CorpusID:31912472)

32. Fuard D, Tzvetkova-Chevolleau T, Decossas S et al (2008) Optimization of poly-di-methyl-siloxane (PDMS) substrates for studying cellular adhesion and motility. Microelectron Eng 85(5–6):1289–1293. https://doi.org/10.1016/j.mee.2008.02.004

33. Murase H, Nanishi K, Kogure H et al (1994) Interactions between heterogeneous surfaces of polymers and water. J Appl Polym Sci 54(13):2051–2062. https://doi.org/10.1002/app.1994.070541307

34. Murase H, Nanishi K (1985) On the relationship of thermodynamic and physical properties of polymers with ice adhesion. Ann Glaciol 6:146–149. https://doi.org/10.1017/S026030550001020X

35. Yamaguchi M, Suzuki S, Sasaki S et al (2014) Fabrication of nano-periodic structures and modification of the Wenzel model to estimate contact angle. Sens Actuators A Phys 212:87–92. https://doi.org/10.1016/j.sna.2014.03.006

36. Sas I, Gorga RE, Joines JA et al (2012) Literature review on superhydrophobic self-cleaning surfaces produced by electrospinning. J Polym Sci B Polym Phys 50(12):824–845. https://doi.org/10.1002/polb.23070

37. Barghi F, Entezari M, Chini SF et al (2020) Effect of initial wetting state on plastron recovery through heating. Int J Heat Mass Transf 156:119705. https://doi.org/10.1016/j.ijheatmasstransfer.2020.119705

38. Gaddam A, Sharma H, Karkantonis T et al (2021) Anti-icing properties of femtosecond laser-induced nano and multiscale topographies. Appl Surf Sci 552:149443. https://doi.org/10.1016/j.apsusc.2021.149443

39. Guo CL, Liu K, Ma CC et al (2024) Constructing a hierarchical coating with photothermal superhydrophobic property by spraying and modification on polyurethane foam for anti-icing and deicing. Appl Therm Eng 236:121907. https://doi.org/10.1016/j.applthermaleng.2023.121

40. Zheng HK, Chang SN, Ma GJ et al (2020) Anti-icing performance of superhydrophobic surface fabricated by femtosecond laser composited dual-layers coating. Energy Build 223(1):110175. https://doi.org/10.1016/j.enbuild.2020.110175

41. Tong W, Cui LL, Qiu RX et al (2021) Laser textured dimple-patterns to govern the surface wettability of superhydrophobic aluminum plates. J Mater Sci Technol 89:59–67. https://doi.org/10.1016/j.jmst.2021.01.084

42. Zhang WY, Gao NJ, Li JW et al (2023) Enhanced anti-icing and anticorrosion properties of nano-SiO2 composite superhydrophobic coating constructed by a large-scale micropillar array approach. Prog Org Coat 175:107324. https://doi.org/10.1016/j.porgcoat.2022.107324

43. Chen XD, Hu LN, Du YZ (2022) Anti-icing and anti-frost properties of structured superhydrophobic coatings based on aluminum honeycombs. Mater Chem Phys 291:126683. https://doi.org/10.1016/j.matchemphys.2022.126683

44. Ge CF, Yuan G, Guo CL et al (2021) Femtosecond laser fabrication of square pillars integrated Siberian-Cocklebur-like microstructures surface for anti-icing. Mater Des 204(13):109689. https://doi.org/10.1016/j.matdes.2021.109689

45. Guo P, Zeng YM, Wen MX et al (2012) Icephobic/anti-icing properties of micro-nano structuresd surfaces. Adv Mater 24(19):2642–2648. https://doi.org/10.1002/adma.201104412

46. Zhang KQ, Xu F, Gao YF (2021) Superhydrophobic and oleophobic dual-function coating with durablity and self-healing property based on a waterborne solution. Appl Mater Today 22(28):100970. https://doi.org/10.1016/j.apmt.2021.100970

47. Liu EY, Zhu G, Dai PZ (2022) Preparation of self-healing Ni-Al layered double hydroxide superhydrophobic coating with nanowall arrays on aluminum alloy. Colloids Surf A Physicochem Eng Asp 652:129916. https://doi.org/10.1016/j.colsurfa.2022.129916

48. Li XL, Liu YJ, Leng JS (2023) Large-scale fabrication of superhydrophobic shape memory composite films for efficient anti-icing and de-icing. Sustain Mater Technol 37:e00692. https://doi.org/10.1016/j.susmat.2023.e00692

Zhao *et al. Surface Science and Technology*   (2024) 2:2

Page 24 of 24

49. Li SY, Zhao F, Bai YP et al (2022) Slippery liquid-infused microphase separation surface enables highly robust anti-fouling, anti-corrosion, anti-icing and anti-scaling coating on diverse substrates. Chem Eng J 431(1):133945. https://doi.org/10.1016/j.cej.2021.133945

50. Qian H, Liu B, Wu D et al (2021) Facile fabrication of slippery lubricant-infused porous surface with pressure responsive property for anti-icing application. Colloids Surf A Physicochem Eng Asp 618(74):126457. https://doi.org/10.1016/j.colsurfa.2021.126457

51. Wong TS, Kang S, Tang S et al (2011) Bioinspired self-repairing slippery surfaces with pressure-stable omniphobicity. Nature 477:443–447. https://doi.org/10.1038/nature10447

52. Prakash CGJ, Prasanth R (2020) Recent trends in fabrication of nepenthes inspired SLIPs: design strategies for self-healing efficient anti-icing surfaces. Surf Interfaces 21:100678. https://doi.org/10.1016/j.surfin.2020.100678

53. Xiang HY, Yuan Y, Zhu T et al (2023) A novel durable anti-icing slippery surfaces with dendritic porous structure. Mater Today Phys 35:101137. https://doi.org/10.1016/j.mtphys.2023.101137

54. Sun XD, Damle VG, Liu SLZ et al (2015) Bioinspired stimuli-responsive and antifreeze-secreting anti-icing coatings. Adv Mater Interfaces 2(5):1400479. https://doi.org/10.1002/admi.201400479

55. Lu JX, Wu SL, Liang ZH et al (2021) Brushable lubricant-infused porous coating with enhanced stability by one-step phase separation. ACS Appl Mater Interfaces 13(19):23134–23141. https://doi.org/10.1021/acsami.1c02751

56. Liang ZH, Liang ZH, Wu SL, Liu C et al (2021) When SLIPS meets TIPS: an endogenous lubricant-infused surface by taking the diluent as the lubricant. Chem Eng J 425:130600. https://doi.org/10.1016/j.cej.2021.130600

57. He Z, Wu C, Hua M et al (2020) Bioinspired multifunctional anti-icing hydrogel. Matter 2(3):723–734. https://doi.org/10.1016/j.matt.2019.12.017

58. Li T, Ibáez-Ibáez PF, Hkonsen V et al (2020) Self-deicing electrolyte hydrogel surfaces with Pa-level ice adhesion and durable antifreezing/antifrost performance. ACS Appl Mater Interfaces 12(31):35572–35578. https://doi.org/10.1021/acsami.0c06912

59. Gao Y, Qi H, Fan D et al (2022) Beetle and mussel-inspired chimeric protein for fabricating anti-icing coating. Colloids Surf B Biointerfaces 210:112252. https://doi.org/10.1016/j.colsurfb.2021.112252

60. Tian JW, Qi X, Li CG et al (2023) Mussel-inspired fabrication of an environment-friendly and self-adhesive superhydrophobic polydopamine coating with excellent mechanical durability, anti-icing and self-cleaning performances. ACS Appl Mater Interfaces 15(21):26000–26015. https://doi.org/10.1021/acsami.3c03577

61. Tian S, Li RQ, Liu XM et al (2023) Inhibition of defect-induced ice nucleation, propagation, and adhesion by bioinspired self-healing anti-icing coatings. Research 6:0140. https://doi.org/10.34133/research.0140

62. Peyman I, Abdullah A-B, Bahareh E et al (2019) Stress-localized durable icephobic surfaces. Mater Horiz 6(4):758–766. https://doi.org/10.1039/C8MH01291A

63. Golovin K, Kobaku SPR, Lee DH et al (2016) Designing durable icephobic surfaces. Sci Adv 2(3):e1501496. https://doi.org/10.1126/sciadv.1501496

64. Jamil MI, Zhan X, Chen F et al (2019) Durable and scalable candle soot icephobic coating with nucleation and fracture mechanism. ACS Appl Mater Interfaces 11(34):31532–31542. https://doi.org/10.1021/acsami.9b09819

65. He Z, Zhuo Y, He J et al (2018) Design and preparation of sandwich-like polydimethylsiloxane (PDMS) sponges with super-low ice adhesion. Soft Matter 14(23):4846–4851. https://doi.org/10.1039/c8sm00820e

66. Jiang X, Lin YW, Xuan XW et al (2023) Stiffening surface lowers ice adhesion strength by stress concentration sites. Colloids Surf A Physicochem Eng Asp 666:131–334. https://doi.org/10.1016/j.colsurfa.2023.131334

67. Chen C, Fan P, Zhu D et al (2023) Crack-initiated durable low-adhesion trilayer icephobic surfaces with microcone-array anchored porous sponges and polydimethylsiloxane cover. ACS Appl Mater Interfaces 15(4):6025–6034. https://doi.org/10.1021/acsami.2c15483

68. Wang ZLL, Zhao ZH, Wen G et al (2023) Fracture-promoted ultraslippery ice detachment interface for long-lasting anti-icing. ACS Nano 17(14):13724–13733. https://doi.org/10.1021/acsnano.3c03023

69. Masoudi A, Irajizad P, Farokhnia N et al (2017) Antiscaling magnetic slippery surfaces. ACS Appl Mater Interfaces 9(24):21025–21033. https://doi.org/10.1021/acsami.7b05564

70. Vasileiou, Thomas, Schutzius et al (2017) Imparting icephobicity with substrate flexibility. Langmuir 33(27):6708–6718. https://doi.org/10.1021/acs.langmuir.7b01412

71. Emelyanenko AM, Boinovich LB et al (2017) Reinforced superhydrophobic coating on silicone rubber for longstanding anti-icing performance in severe conditions. ACS Appl Mater Interfaces 9(28):24210–24219. https://doi.org/10.1021/acsami.7b05549

72. Golovin K, Dhyani A, Thouless MD et al (2019) Low-interfacial toughness materials for effective large-scale deicing. Science 364(6438):371–375. https://doi.org/10.1126/science.aav1266

73. Liu ZY, Hu JH, Guo L et al (2022) Superhydrophobic and photothermal deicing composite coating with self-healing and anti-corrosion for anti-icing applications. Surf Coat Technol 444:128668. https://doi.org/10.1016/j.surfcoat.2022.128668

74. Lin ZM, Ma C, Ma Z et al (2023) Laser etching ultra-black coating with novel anti-icing performance. Chem Eng J 466:143067. https://doi.org/10.1016/j.cej.2023.143067

75. Yu B, Sun Z, Liu Y et al (2023) Photo-thermal superhydrophobic sponge for highly efficient anti-icing and de-icing. Langmuir 39(4):1686–1693. https://doi.org/10.1021/acs.langmuir.2c03384

76. Lee SH, Kim J, Seong M et al (2022) Magneto-responsive photothermal composite cilia for active anti-icing and de-icing. Compos Sci Technol 217:109086. https://doi.org/10.1016/j.compscitech.2021.109086

77. Liu YB, Guo RY, Liu J et al (2023) Robust PFMA/CNTs composite PDMS superhydrophobic film via SI-CuCRP method for efficient anti-icing. Colloids Surf A Physicochem Eng Asp 660:130913. https://doi.org/10.1016/j.colsurfa.2022.130913

78. Guo H, Liu M, Xie C et al (2020) A sunlight-responsive and robust anti-icing/deicing coating based on the amphiphilic materials. Chem Eng J 402(1):126161. https://doi.org/10.1016/j.cej.2020.126161

79. Sullivan A, Duan XL, Yang JM (2023) Energy-efficient anti-icing performance of a hybrid superhydrophobic and electrothermal coating on metallic substrates. Mater Chem Phys 301:127700. https://doi.org/10.1016/j.matchemphys.2023.127700

80. Wang Z, Shen YZ, Tao J et al (2023) An integrated superhydrophobic anti/de-icing film heater with low energy consumption: Interpenetration behavior of components based on wet-film spraying method. Appl Therm Eng 223(2):120028. https://doi.org/10.1016/j.applthermaleng.2023.120028

81. Zeng D, Li Y, Liu HQ et al (2023) Superhydrophobic coating induced anti-icing and deicing characteristics of an airfoil. Colloids Surf A Physicochem Eng Asp 660:130824. https://doi.org/10.1016/j.colsurfa.2022.130824

82. Chen J, Marklund P, Björling M et al (2023) In-situ polymerized siloxane urea enhanced graphene-based super-fast, durable, all-weather elec-photo-thermal anti-/de-icing coating. J Sci Adv Mater Dev 8(3):100604. https://doi.org/10.1016/j.jsamd.2023.100604

83. Zhao ZH, Chen HW, Zhu YT et al (2022) A robust superhydrophobic anti-icing/de-icing composite coating with electrothermal and auxiliary photothermal performances. Compos Sci Technol 227:109578. https://doi.org/10.1016/j.compscitech.2022.109578

84. Yuan Y, Xiang HY, Liu GY et al (2021) Fabrication of phase change microcapsules and their applications to anti-icing coating. Surf Interfaces 27:101516. https://doi.org/10.1016/j.surfin.2021.101516

85. Shamshiri M, Jafari R, Momen G (2023) A novel hybrid anti-icing surface combining an aqueous self-lubricating coating and phase-change materials. Prog Org Coat 177:107414. https://doi.org/10.1016/j.porgcoat.2023.107414

Publisher's Note